Collision-induced absorption of radiation by interacting molecules

Katharine L. C. Hunt
Department of Chemistry, Michigan State University
Institute for Advanced Studies, Department of Physics and Materials Science, University of Luxembourg

Physics Seminar, November 24, 2023

Interactions between molecules during a collision induce transient dipoles. The interactions break the symmetry of non-dipolar species. The induced dipoles change as the molecules rotate and vibrate, leading to collision-induced absorption in the infrared and far infrared.

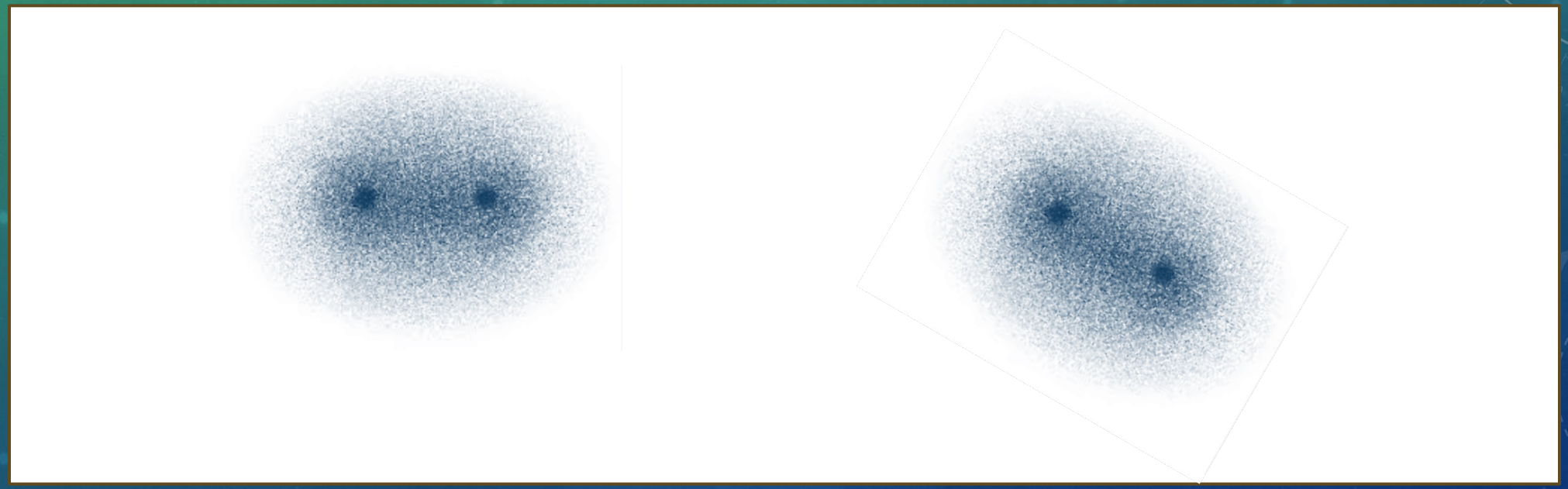

https://www1.eere.energy.gov/hydrogenandfuelcells/tech_validation/pdfs/fcm01r0.pdf

Collision-induced absorption has been extensively studied experimentally at and below room temperature, in samples of hydrogen, nitrogen, methane, and other molecules.

Information on collision-induced dipoles is needed for astrophysical applications.

- Anomalous radiative profile of very old, very cool white dwarf stars.
- Formation of the first stars in the universe?
- Temperature profiles of the outer planets and exoplanets.

Hubble Image

Visible light, NASA/ESA 2014

James Webb Space Telescope Image

Near-infrared, NASA 2022

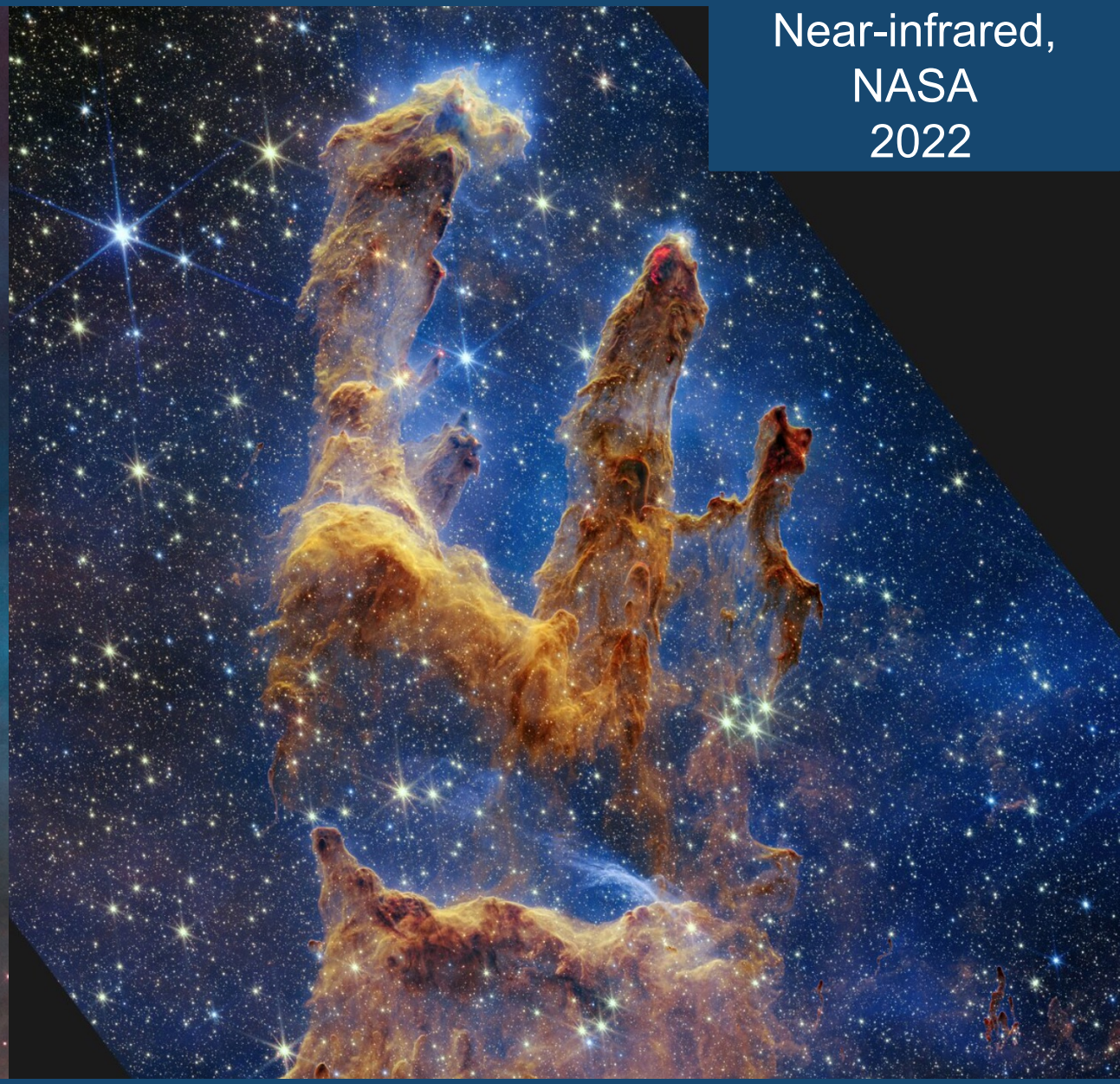

The Pillars of Creation, a star-forming region in the Eagle Nebula

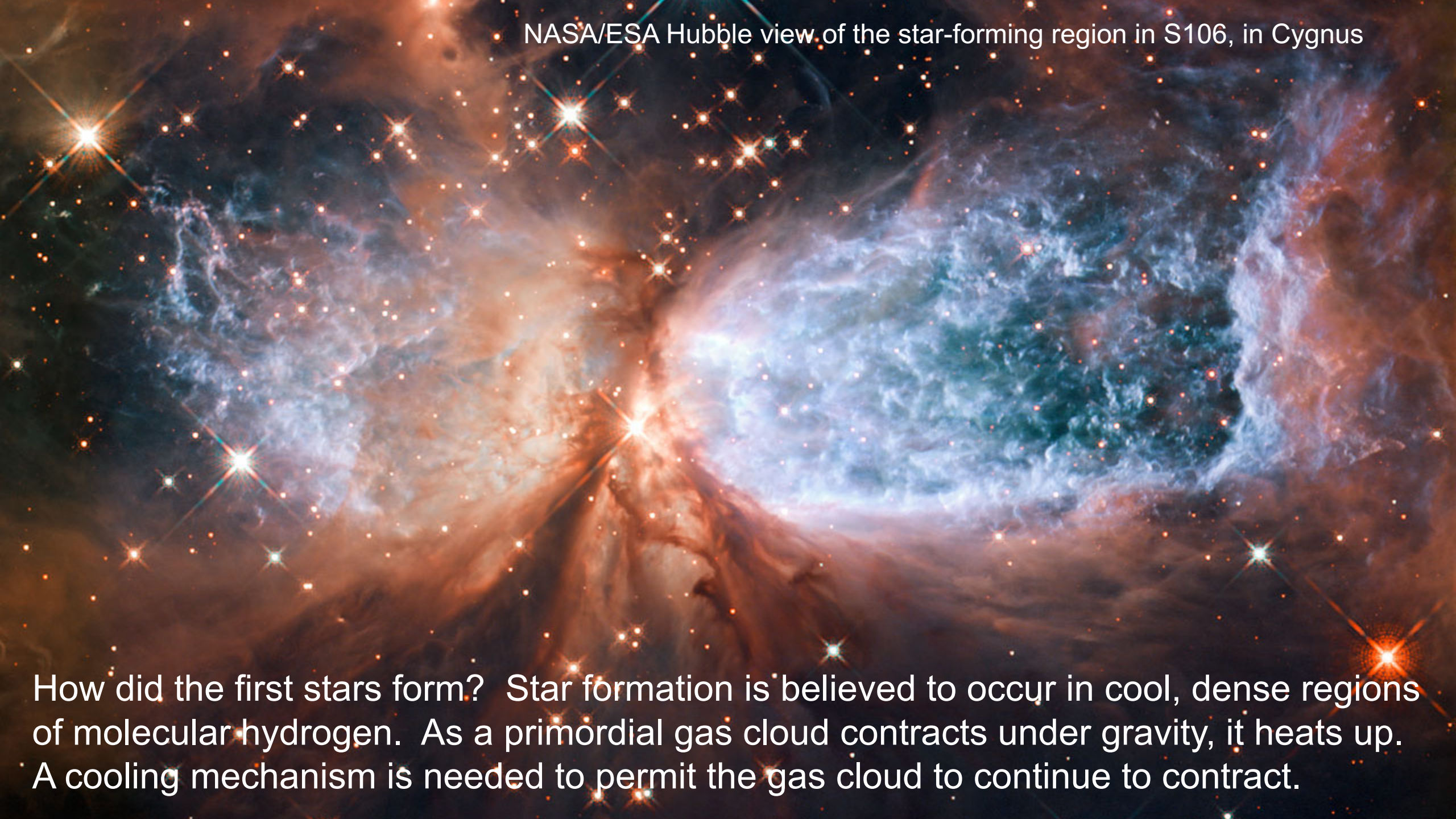

NASA/ESA Hubble view of the star-forming region in S106, in Cygnus

How did the first stars form? Star formation is believed to occur in cool, dense regions of molecular hydrogen. As a primordial gas cloud contracts under gravity, it heats up. A cooling mechanism is needed to permit the gas cloud to continue to contract.

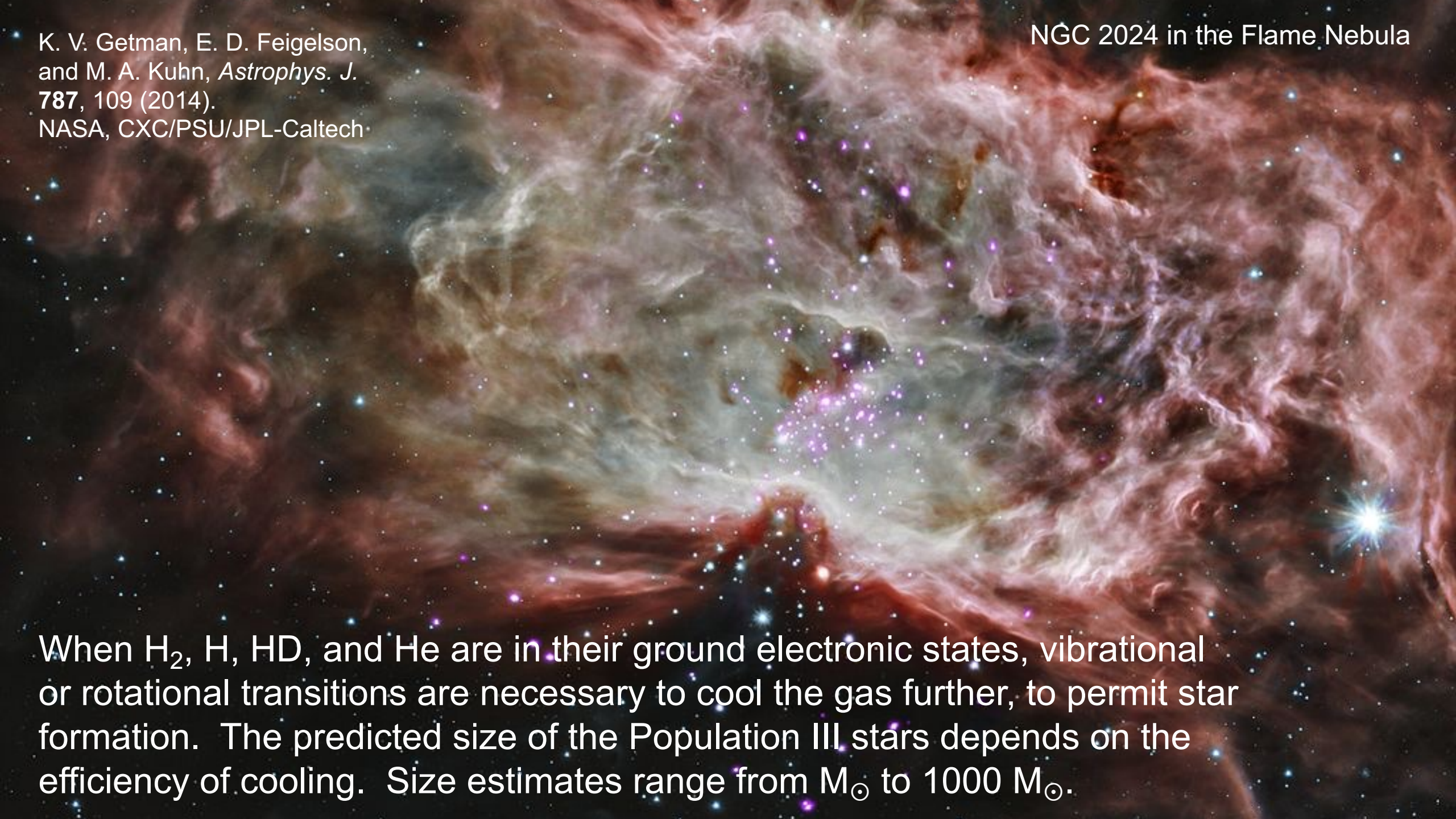

K. V. Getman, E. D. Feigelson, and M. A. Kuhn, *Astrophys. J.* **787**, 109 (2014).
NASA, CXC/PSU/JPL-Caltech

NGC 2024 in the Flame Nebula

When H_2, H, HD, and He are in their ground electronic states, vibrational or rotational transitions are necessary to cool the gas further, to permit star formation. The predicted size of the Population III stars depends on the efficiency of cooling. Size estimates range from $M_\odot$ to 1000 $M_\odot$.

Further Astrophysical uses of information on H, He, and H_2 interactions
Dynamical modeling, radiation profiles, cooling rates

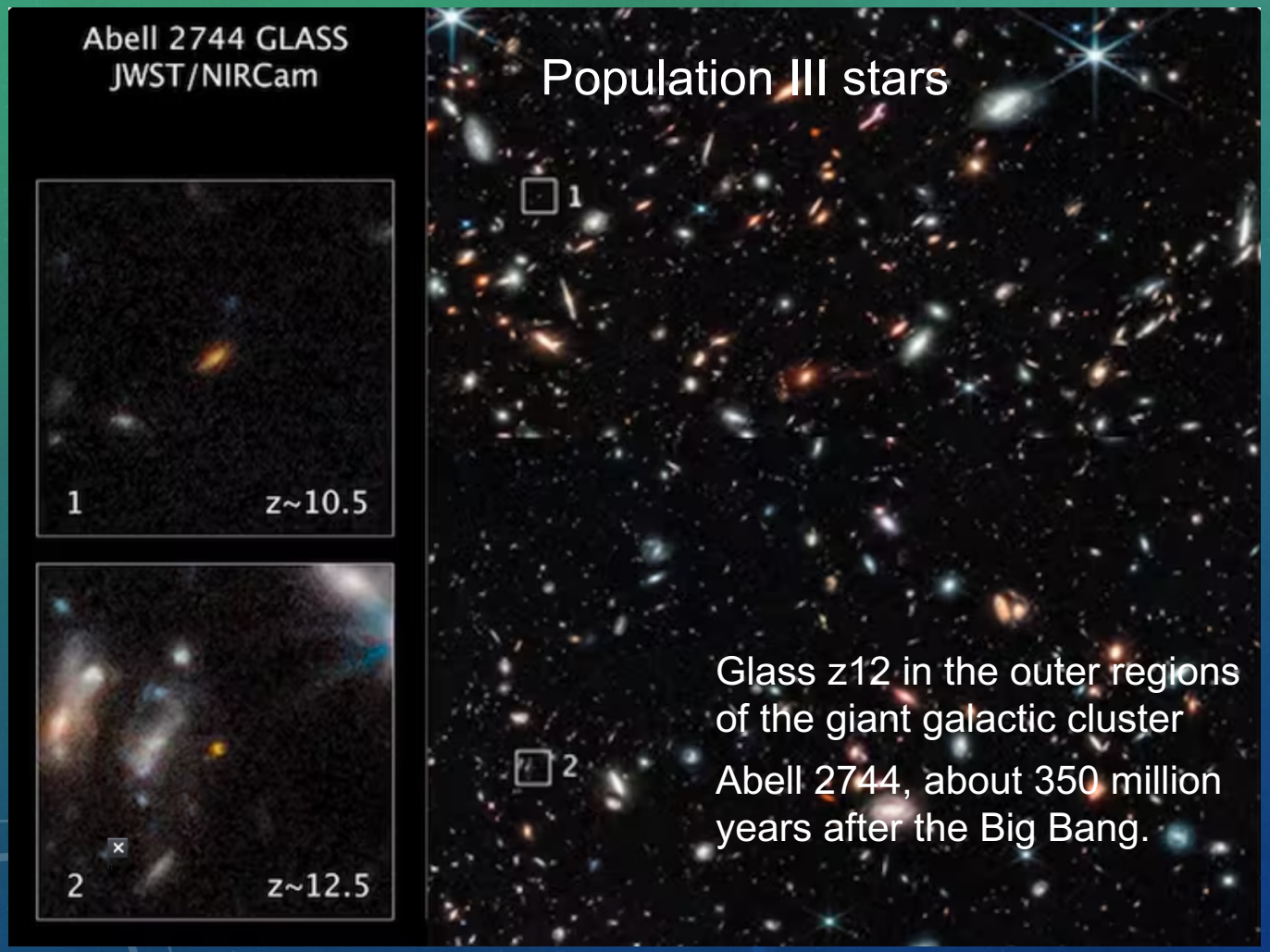

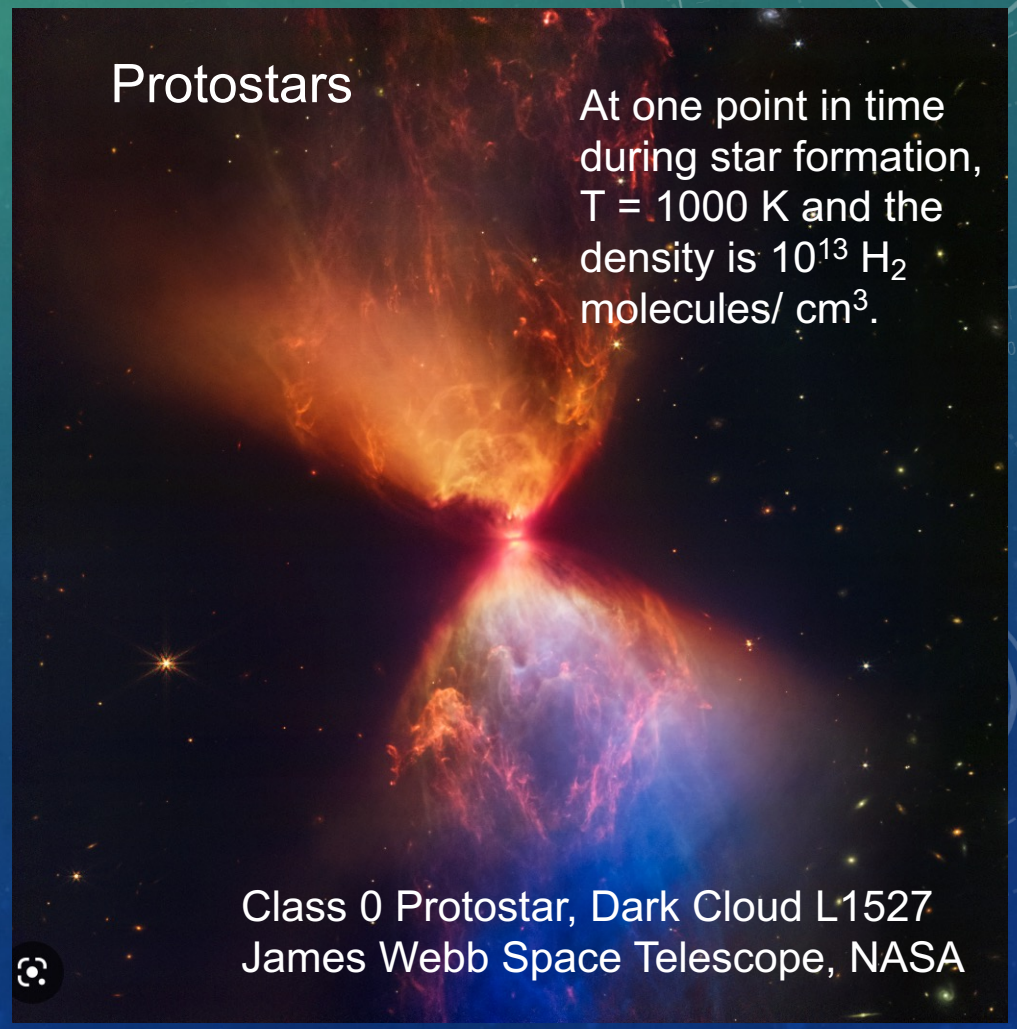

Gas giants and gas giant exoplanets

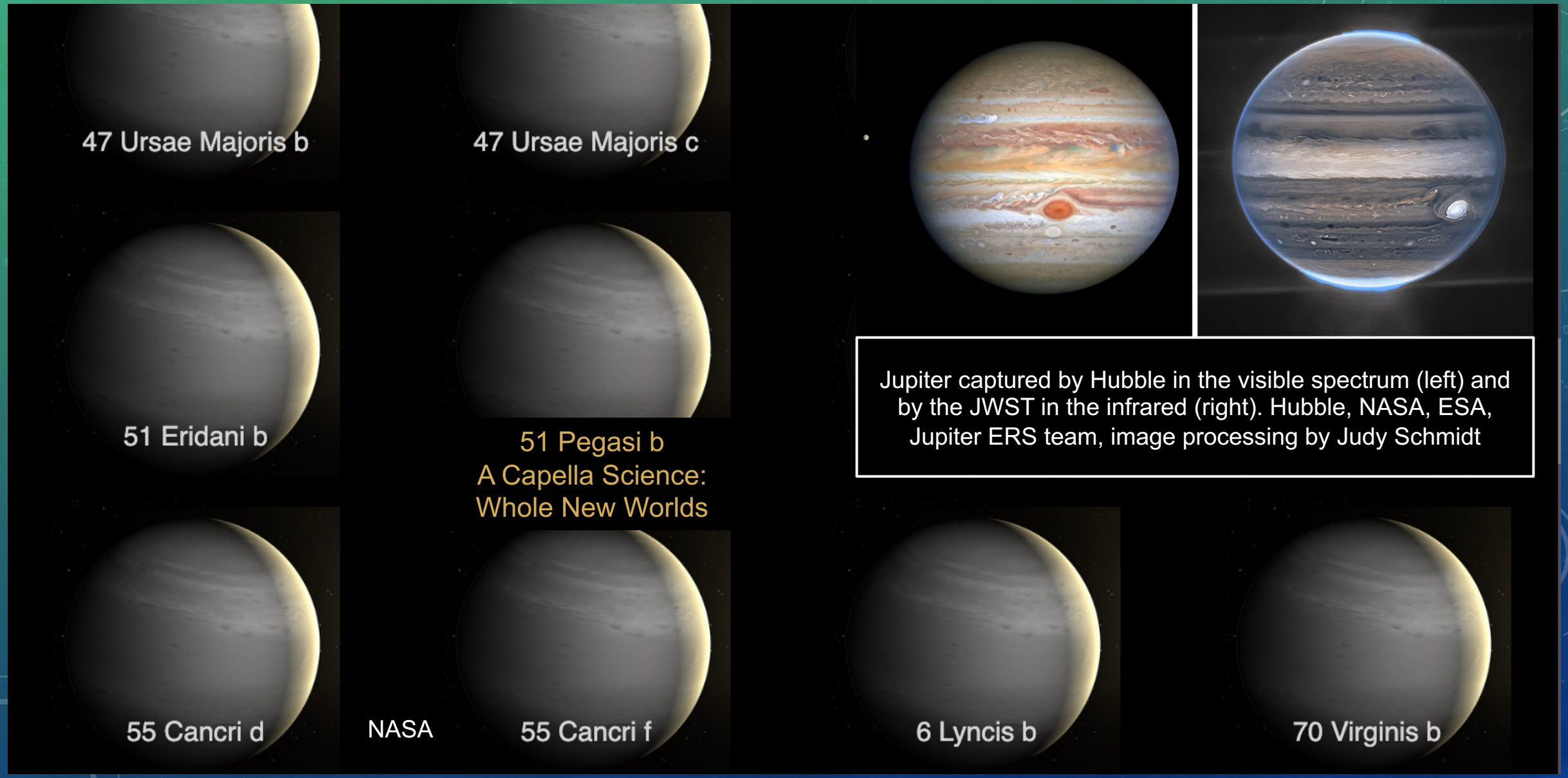

Jupiter captured by Hubble in the visible spectrum (left) and by the JWST in the infrared (right). Hubble, NASA, ESA, Jupiter ERS team, image processing by Judy Schmidt

Collision-induced absorption by H_2 gas near room temperature

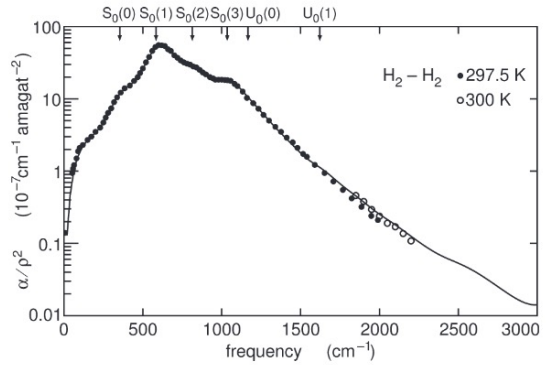

Figure 2. Collision-induced absorption by pairs of H_2 molecules in the rotational band of H_2 in hydrogen gas at room temperature. Calculation: solid trace. Measurements: dots[37] and circles.[38]

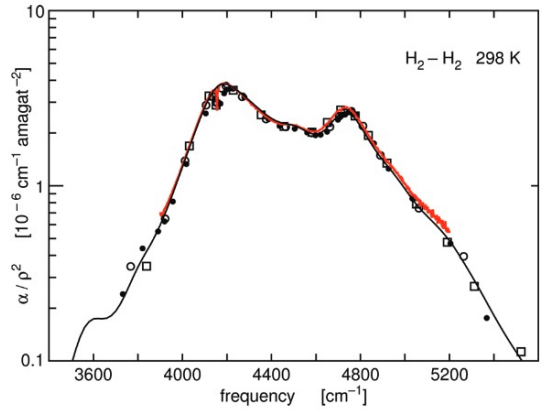

Figure 3. Collision-induced absorption by pairs of H_2 molecules in the fundamental band of H_2 in hydrogen gas at room temperature. Calculation: solid (smooth) trace. Measurements: dots,[39,40] circles,[41] squares,[42] red trace (slightly noisy).[43]

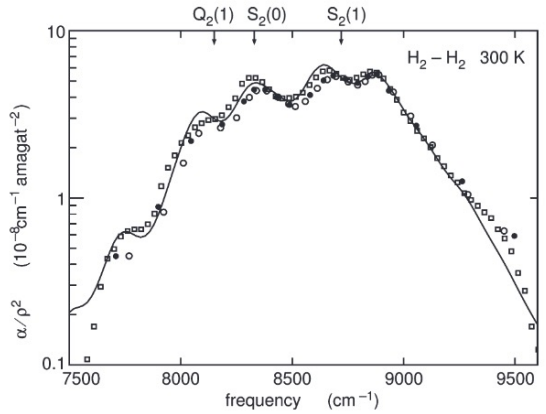

Figure 4. Collision-induced absorption by pairs of H_2 molecules in the first overtone band of H_2 at room temperature in hydrogen gas. Calculation: solid trace. Measurements: open squares,[2] dots,[40] circles.[44]

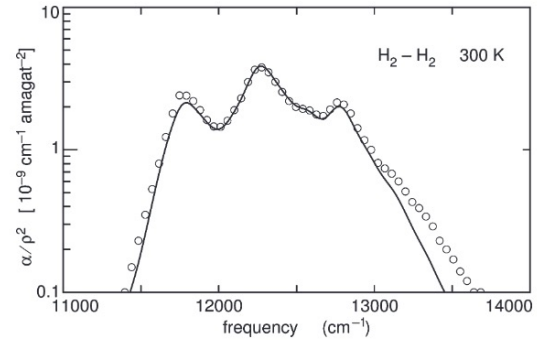

Figure 5. Collision-induced absorption by pairs of H_2 molecules in the second overtone band of H_2 at room temperature in hydrogen gas. Calculation (solid line). Measurement: circles.[49]

Comparison of experimental and calculated spectra

Figure 2: Rotational band
Figure 3: Fundamental vibrational band
Figure 4: First vibrational overtone
Figure 5: Second vibrational overtone

From: Martin Abel, Lothar Frommhold, Xiaoping Li, and Katharine L. C. Hunt, *J. Phys. Chem. A* **115**, 6805 (2011).

Collision-induced absorption by H_2 gas at lower temperatures

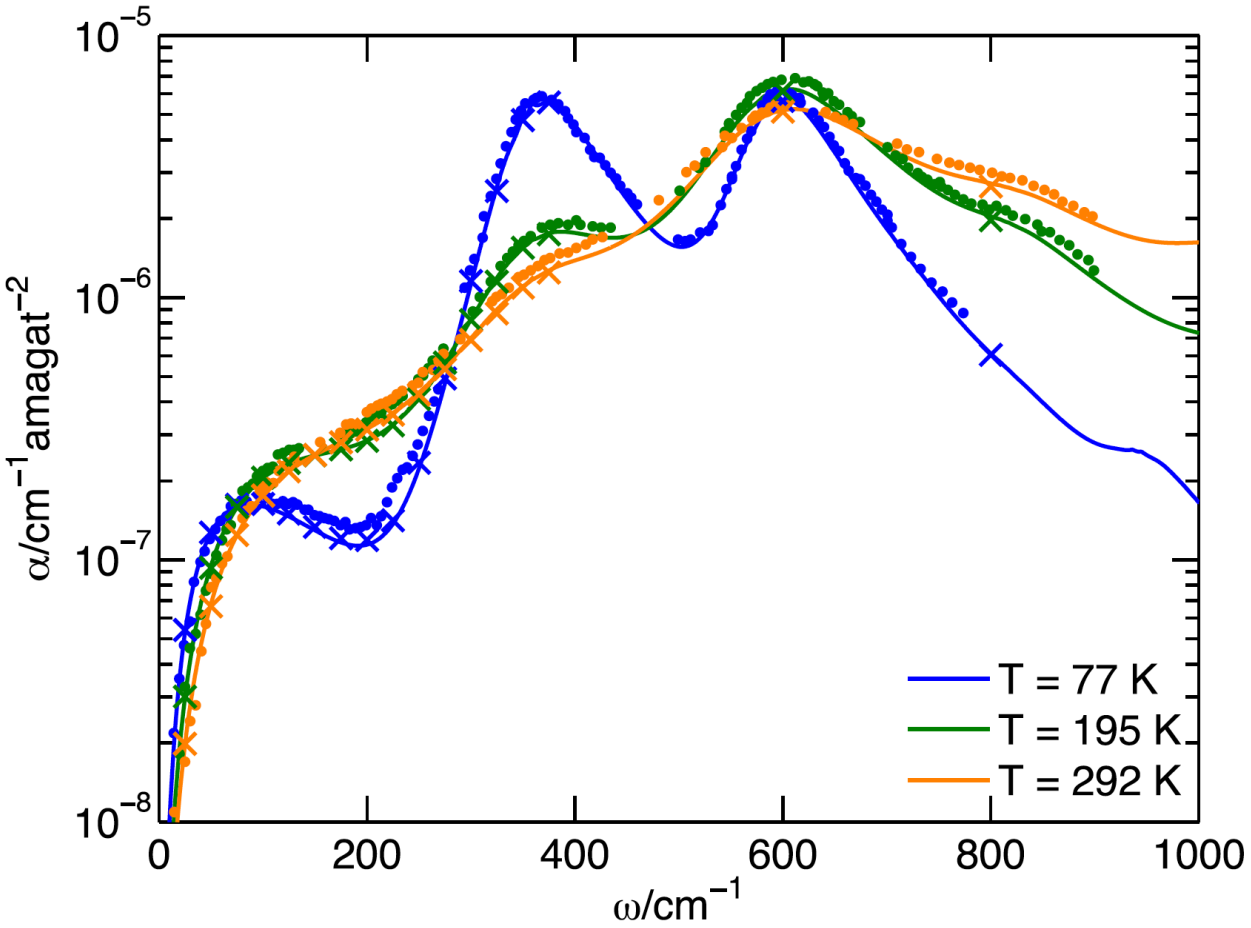

Measurements:

- 77 K
- 195 K
- 292 K

Solid lines:
Isotropic interactions, distinguishable H nuclei

× × ×

Anisotropic potential, indistinguishable H nuclei

T. Karman, A. van der Avoird, and G. C. Groenenboom, *J. Chem. Phys*. **142**, 084305 (2015).

A case with no experiments! Collision-induced dipole of $H_2 \cdots H$

Comparison with previous calculations:
RWP: R. W. Patch, *J. Chem. Phys*. **59**, 6468 (1973).
GFM: M. Gustafsson, L. Frommhold, and W. Meyer, *J. Chem. Phys*. **118**, 1667 (2003).

Work	Method	Basis	# of θ	# of r	# of R
RWP	Full CI	Three 1s	6	1, 1.401446 a.u.	4, from 1 to 4 a.u.
GFM	MCSCF + CEPA with SCEP	75 functions	4 (0º to 90º in 30º intervals)	5 (1.111 to 1.787 a.u.)	11, from 3 to 11 a.u.
Our work	UCCSD(T)/RHF	165 functions	19 (0º to 90º in 5º intervals)	9 (0.942 a.u. to 2.801 a.u.)	16, from 3 to 10 a.u.

H.-K. Lee, X. Li, E. Miliordos, and K. L. C. Hunt, *J. Chem. Phys*. **150**, 204307 (2019).

Finite field methods with 6 fields, base strength f,
Strengths {f, – f , $2^{1/2}$ f, – $2^{1/2}$ f, $3^{1/2}$ f, – $3^{1/2}$ f}
Total of 43, 000 *ab initio* calculations
aug-cc-pV5Z, aug-cc-pV6Z & d-aug-cc-pV5Z basis sets

10^3 | μ_y | (a.u.),
r = 2.125 a.u.

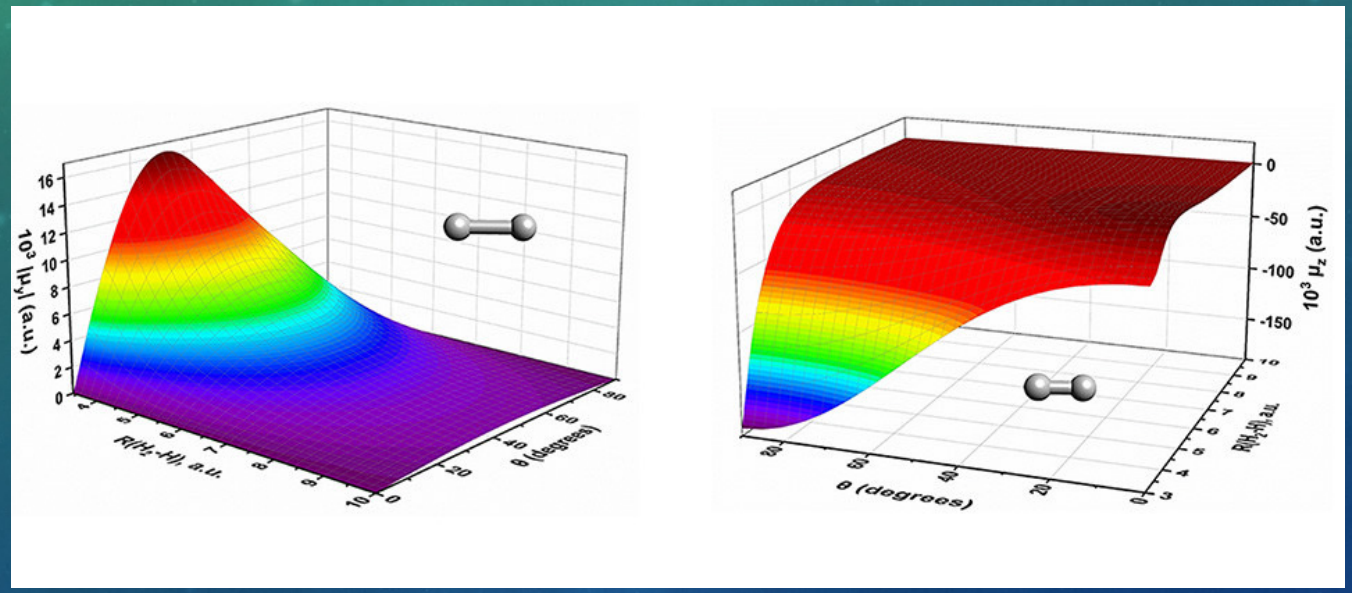

10^3 μ_z (a.u.),
r = 1.449 a.u.

H.-K. Lee, X. Li, E. Miliordos, and K. L. C. Hunt, *J. Chem. Phys*. **150**, 204307 (2019).
Figure by Lee *et al*., in: Adam Liebendorfer; *Scilight* **2019,** 220002 (2019).

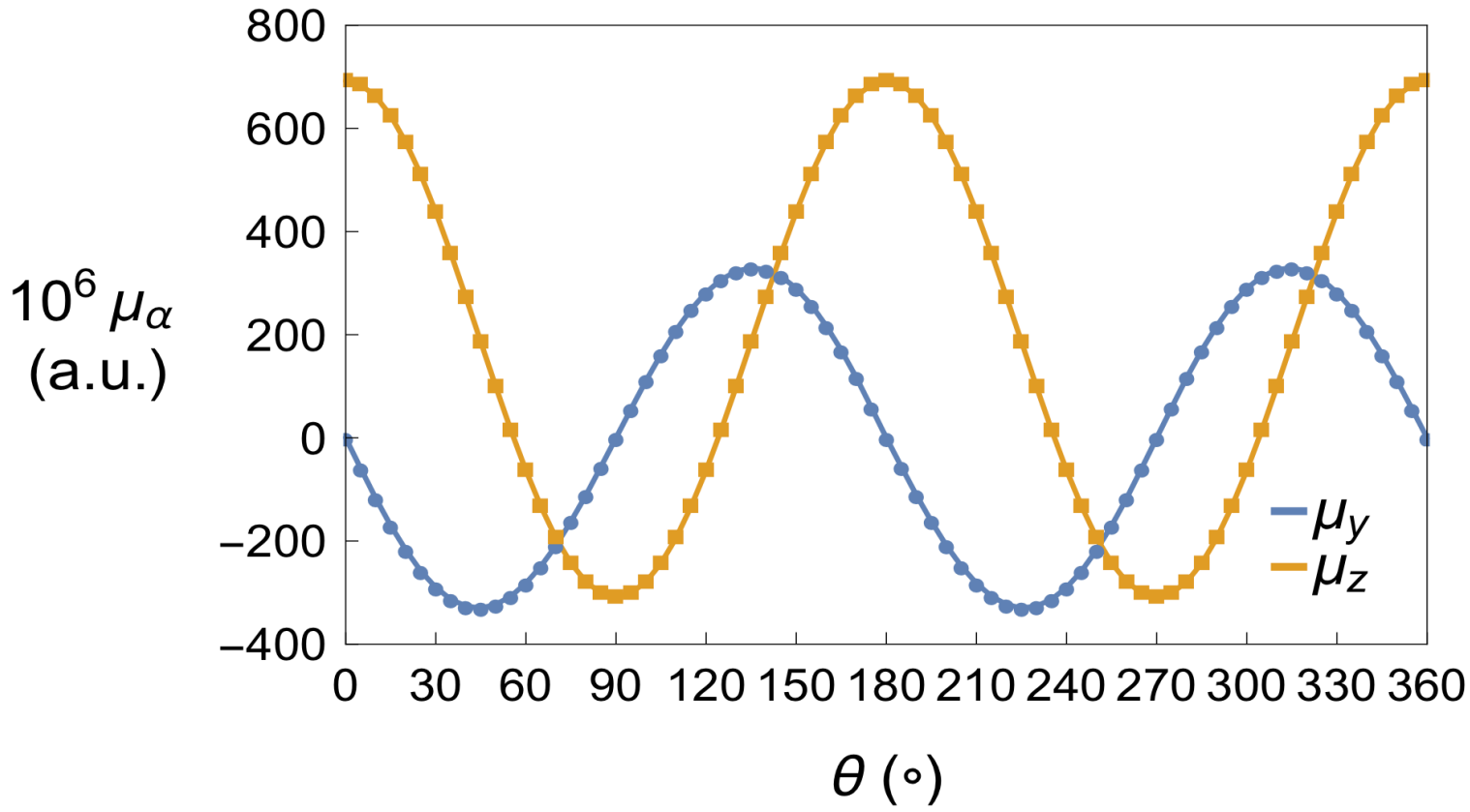

Dipole moments in the y and z directions, as a function of the angle θ between the H_2 bond axis and the intermolecular vector. Results from 0º to 90º from a*b initio* calculations, remainder obtained by symmetry arguments

H.-K. Lee, X. Li, E. Miliordos, and K. L. C. Hunt, *J. Chem. Phys*. **150**, 204307 (2019).

Spherical Tensor Analysis of the Dipole

$$\mu^{M}(r, R, \theta) = 4\pi/3^{1/2} \sum_{\lambda, L, m} D_{\lambda L}(r, R) \langle\ \lambda\ L\ m\ M - m \mid 1\ M \rangle\ Y_{\lambda}^{m}(\theta, \phi)\, Y_{L}^{M-m}(0, 0)$$

Correspondence with Cartesian tensor elements

$$\mu^{0}(r, R, \theta) = \mu_{z}(r, R, \theta)$$

$$\mu^{1}(r, R, \theta) = -(1/2)^{1/2} [\ \mu_{x}(r, R, \theta) + i\, \mu_{y}(r, R, \theta)\ ]$$

$$\mu^{-1}(r, R, \theta) = (1/2)^{1/2} [\ \mu_{x}(r, R, \theta) - i\, \mu_{y}(r, R, \theta)\ ]$$

Advantages: This illuminates the physical mechanisms that contribute to the dipole. This form is also very useful in spectroscopic line shape calculations.

Physical mechanisms of dipole induction for $H_2 \cdots H$

The leading long-range contribution comes from the quadrupole-induced dipole
- This contribution varies as R^{-4} in the separation of H_2 and H
- It shows up in the spherical tensor expansion coefficient D_{23}

Hexadecapolar induction is also apparent in the *ab initio* results
- This contribution varies as R^{-6} in the separation of H_2 and H
- It shows up in the spherical tensor expansion coefficient D_{45}

Dispersion and back-induction are also apparent in the *ab initio* results
- These contributions vary as R^{-7} in the separation of H_2 and H
- They are evident in D_{01}. They are present in other coefficients, but harder to detect there

D_{21} and D_{43} have no long-range classical counterparts, but they contribute significantly at shorter range

Results for Spherical Tensor Components

$$\mu^{M}(r, R, \theta) = 4\pi/3^{1/2} \sum_{\lambda, L, m} D_{\lambda L}(r, R) \langle\, \lambda\ L\ m\ M - m \mid 1\ M \,\rangle\ Y_{\lambda}^{m}(\theta, \phi)\ Y_{L}^{M-m}(0, 0)$$

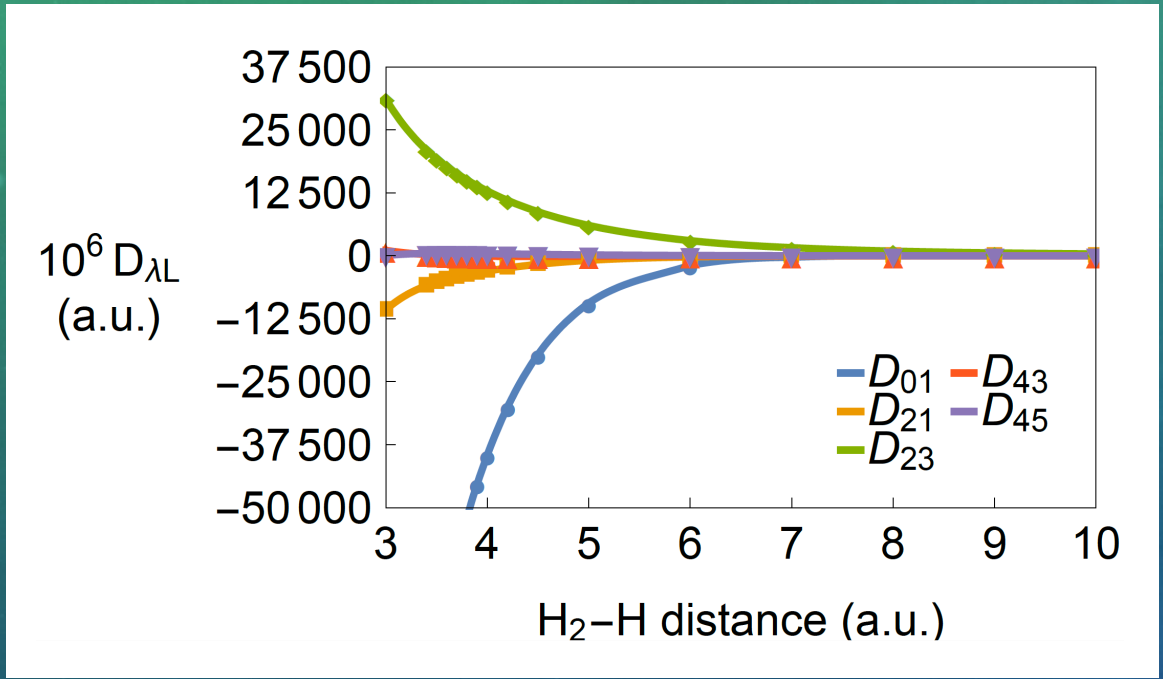

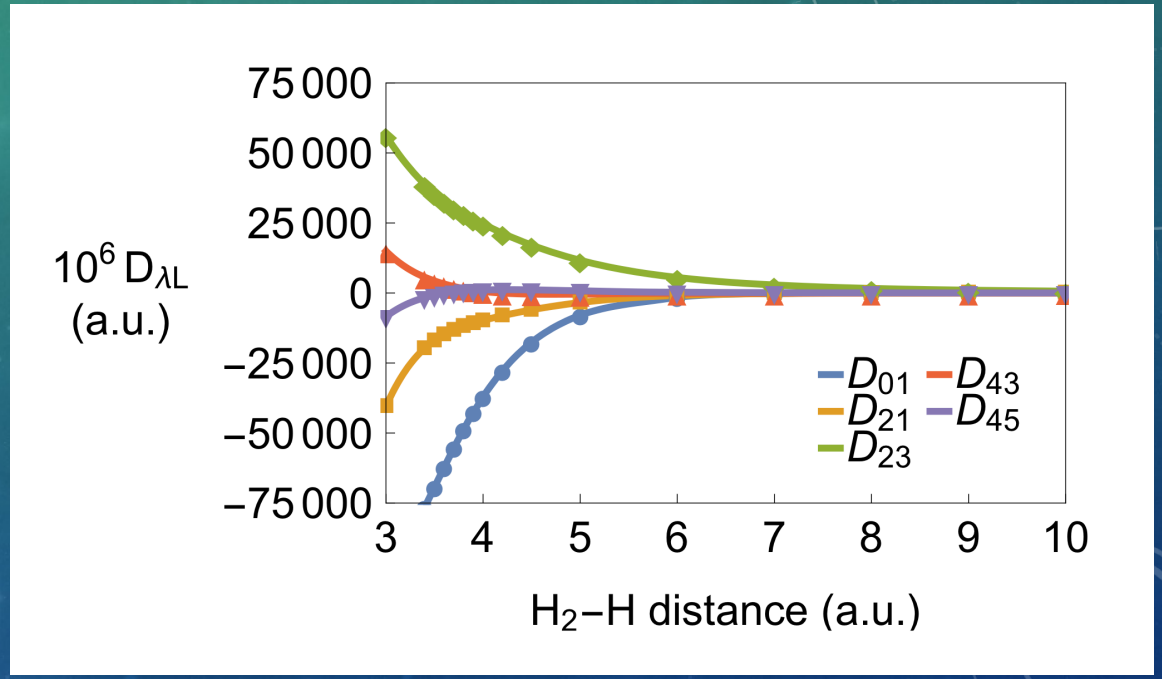

Results for the leading expansion coefficients. The largest coefficients are D_{01} and D_{23}. As the separation R decreases, D_{21}, D_{43}, and D_{45} grow in relative magnitude.

H.-K. Lee, X. Li, E. Miliordos, and K. L. C. Hunt, *J. Chem. Phys.* **150**, 204307 (2019).

Dependence of Spherical Tensor Components on Bond Length

$$\mu^{M}(r, R, \theta) = 4\pi/3^{1/2} \sum_{\lambda, L, m} D_{\lambda L}(r, R) \langle\, \lambda\ L\ m\ M - m \mid 1\ M \,\rangle\ Y_{\lambda}^{m}(\theta, \phi)\ Y_{L}^{M-m}(0, 0)$$

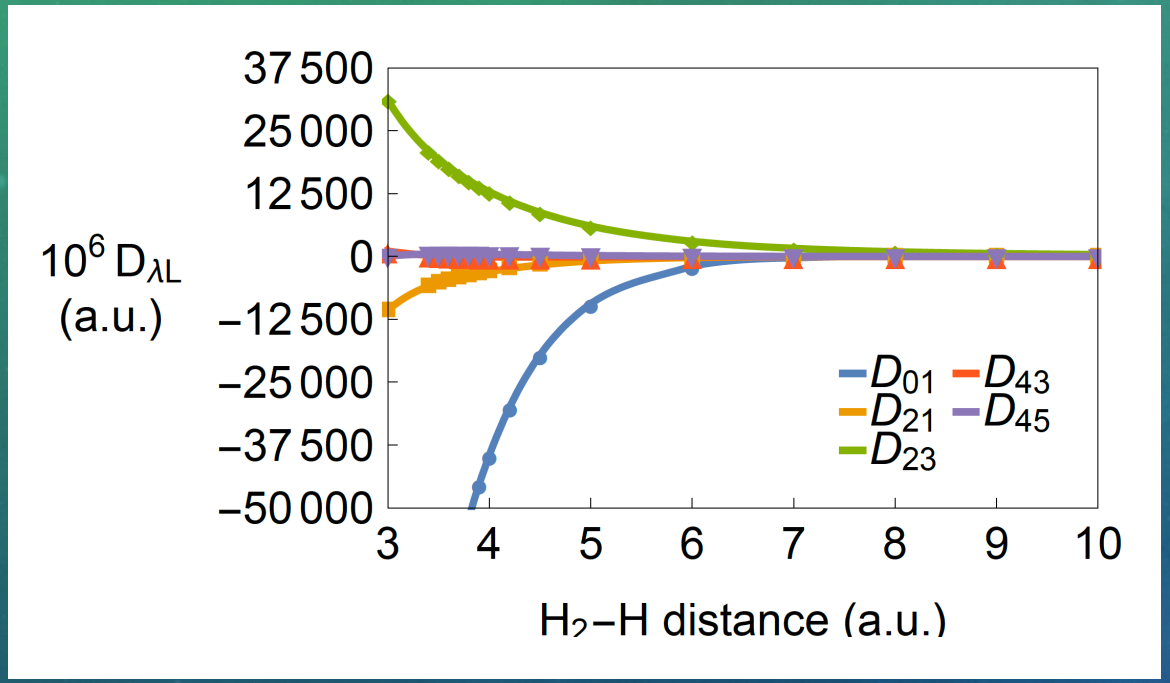

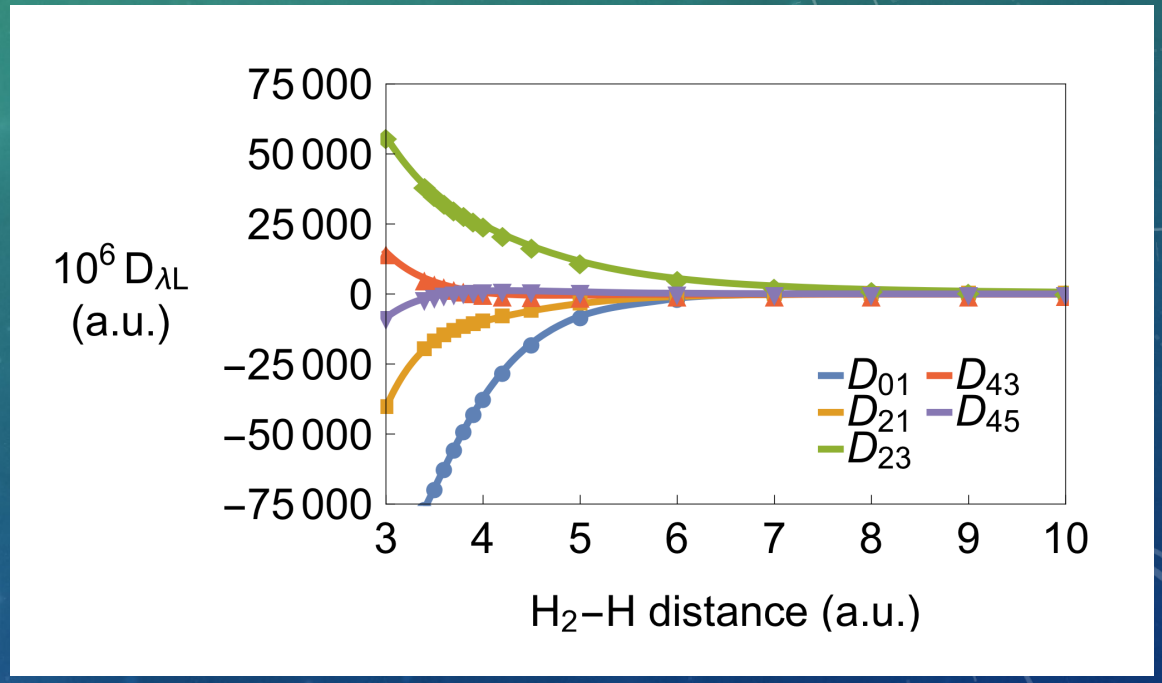

The largest coefficients are D_{01} and D_{23}. As the bond length increases, D_{21}, D_{43}, and D_{45} grow in relative magnitude

H.-K. Lee, X. Li, E. Miliordos, and K. L. C. Hunt, *J. Chem. Phys.* **150**, 204307 (2019).

Comparison with Known Long-Range Forms

$$\mu^{M}(r, R, \theta) = 4\pi/3^{1/2} \sum_{\lambda, L, m} D_{\lambda L}(r, R) \langle\, \lambda\ L\ m\ M - m \mid 1\ M \,\rangle\ Y_{\lambda}^{m}(\theta, \phi)\ Y_{L}^{M-m}(0, 0)$$

Largest coefficients: D_{01} and D_{23}. As r increases, D_{21}, D_{43}, and D_{45} grow.

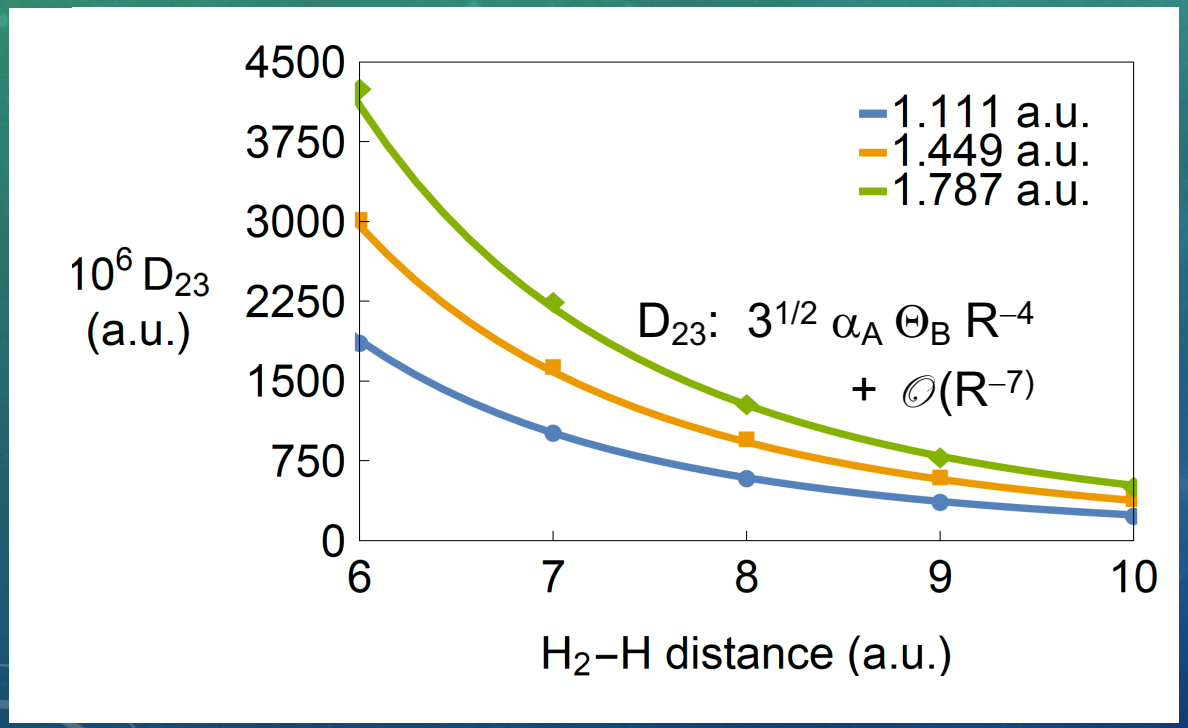

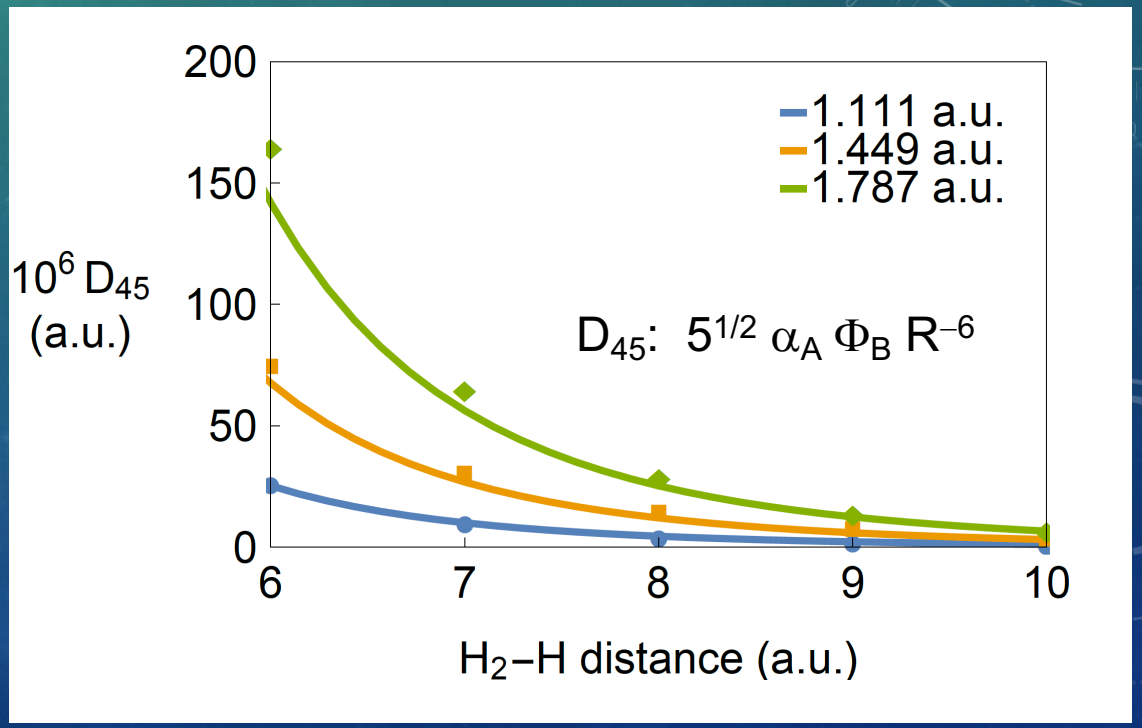

H.-K. Lee, X. Li, E. Miliordos, and K. L. C. Hunt, *J. Chem. Phys.* **150**, 204307 (2019).

Dispersion dipoles of unlike pairs A and B

- $\mu^{AB}_{disp} = -\partial \Delta E^{AB}_{disp} / \partial F \Big|_{F \to 0}$
- Spontaneous, quantum mechanical fluctuations in the charge density of molecule A set up a nonuniform local field at B.

$$F^{A}(\omega) = T^{(2)}(R) \cdot \mu^{A}_{fl}(\omega) + (1/3)\, T^{(3)}(R) : \theta^{A}_{fl}(\omega) + \ldots$$

$$F'^{A}(\omega) = -\, T^{(3)}(R) \cdot \mu^{A}_{fl}(\omega) + \ldots$$

- The local field induces charge moments in B, as determined by the field-dependent susceptibilities of B and the nonuniformity of the local field.

Reaction field theory for ΔE_{vdW}:

B. Linder, *Adv. Chem. Phys*. **12**, 225 (1967).

D. Langbein, *Theory of van der Waals Attraction* (Springer, New York, 1974) Chapter 3.

Theory of the dispersion dipole:

K. L. C. Hunt and J. E. Bohr, *J. Chem. Phys*. **83**, 5198 (1985).

- The Induced dipole is

$$\mu^{B}_{ind}(\omega) = \alpha^{B}(F, \omega) \cdot F^{A}(\omega) + (1/3)\, A^{B}(F, \omega) : F'^{A}(\omega) + (1/\omega)\, G'^{B}(F, \omega) \cdot B^{A}(\omega) + \ldots$$

- The induced polarization in B gives rise to a nonuniform local field at A, the reaction field:

$$F^{B}(\omega) = T^{(2)}(R) \cdot \mu^{B}_{ind}(\omega) - (1/3)\, T^{(3)}(R) : \theta^{B}_{ind}(\omega) + \ldots$$

$$F'^{B}(\omega) = T^{(3)}(R) \cdot \mu^{B}_{ind}(\omega) + \ldots$$

- The resulting change in the energy of molecule A is the average of the instantaneous energy shift over fluctuating charge distribution of A.

$$\Delta E^{A} = -(1/2) \langle\, \mu^{A}_{fl}(t) \cdot F^{B}(t) \,\rangle - (1/6) \langle\, \theta^{A}_{fl}(t) : F'^{B}(t) \,\rangle + \ldots$$

- The field and field gradients from B result from the spontaneously fluctuating multipoles of A. Their correlations are given by the fluctuation-dissipation theorem, applied to A in the field F.

- From the fluctuation-dissipation theorem of H. B. Callen and T. Welton, *Phys. Rev*. **83**, 34 (1951), modified for static-field effects,

$$(1/2)\,\langle\, \mu_\alpha(\omega)\,\mu_\beta(\omega') + \mu_\beta(\omega')\,\mu_\alpha(\omega)\,\rangle_F$$

$$= (\hbar/2\pi)\,\alpha\,''_{\alpha\beta}(\omega; F)\,\delta(\omega + \omega')\coth(\hbar\omega/2kT)$$

$$(1/2)\,\langle\, \mu_\alpha(\omega)\,\theta_{\beta\gamma}(\omega') + \theta_{\beta\gamma}(r', \omega')\,\mu_\alpha(\omega)\,\rangle_F$$

$$= (\hbar/2\pi)\,A''_{\alpha,\beta\gamma}(r, r', \omega; F)\,\delta(\omega + \omega')\coth(\hbar\omega/2kT)$$

- The effects of a spontaneous fluctuation in the charge density of B are added.
- The net energy change is given in terms of an integral over all real frequencies.
- The real parts of the susceptibilities are even in the frequency, and the imaginary parts are odd. This permits us to write the energy change as the integral over an analytic function of ω.

- The susceptibilities are analytic in the upper half plane, to ensure causality. Therefore, the only poles in the upper half plane come from the function $\coth(\hbar\omega/2kT)$. They are located along the imaginary axis at $\omega_n = 2\pi i\, nkT/\hbar$.

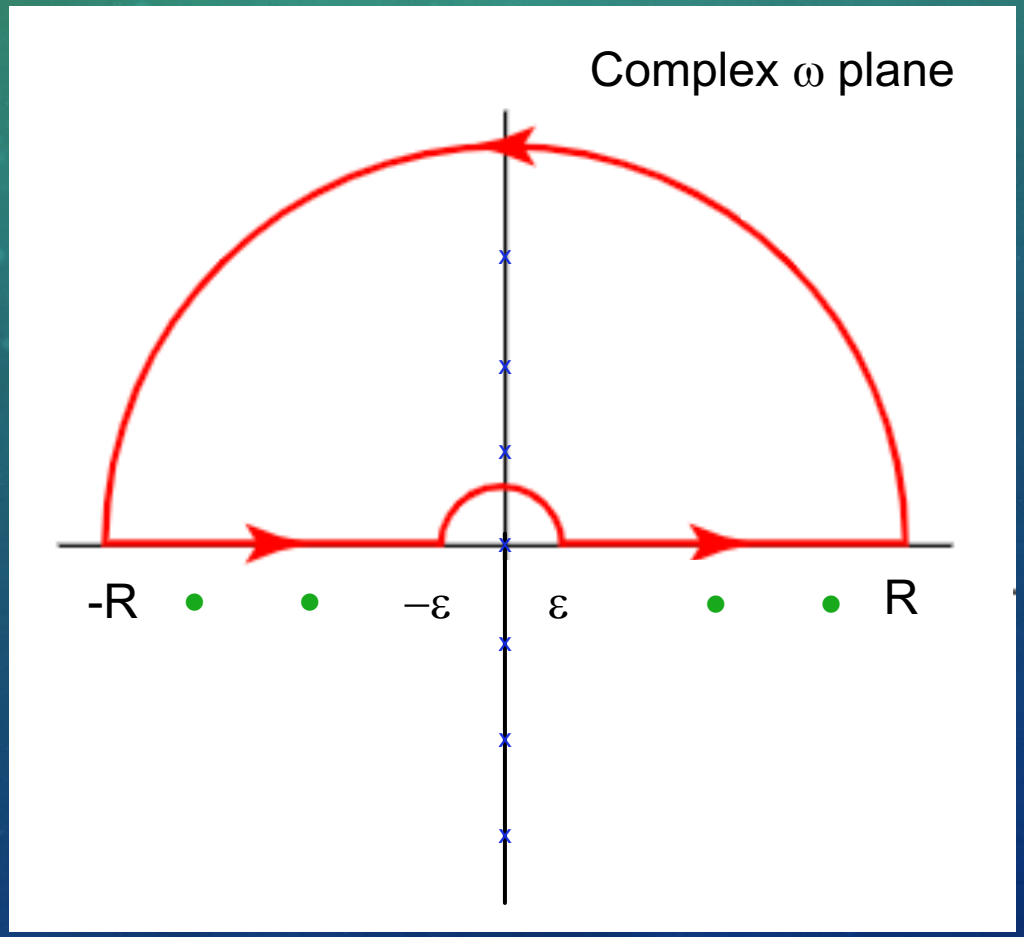

- Typically, the poles along the imaginary axis are sufficiently close together that the sum over the poles can be converted to an integral over imaginary frequencies.
- Then expand the susceptibilities in the field F, to obtain the answer

Result for the dispersion dipole of atoms or centrosymmetric molecules:

$$\mu_\phi^{AB} = (\hbar/3\pi) \int_0^\infty d\omega \; T^{(2)}_{\alpha\beta}(R) \; \alpha^B_{\beta\gamma}(i\omega) \; T^{(3)}_{\gamma\delta\varepsilon}(R) \; B^A_{\alpha\phi,\delta\varepsilon}(0, i\omega)$$
$$- T^{(2)}_{\alpha\beta}(R) \; B^B_{\beta\phi,\gamma\delta}(0, i\omega) \; T^{(3)}_{\gamma\delta\varepsilon}(R) \; \alpha^A_{\varepsilon\alpha}(i\omega)$$

$\alpha_{\alpha\beta}(i\omega)$

$B_{\alpha\beta,\gamma\delta}(0, i\omega)$

$T^{(2)}_{\alpha\beta}(R) = \nabla_\alpha \nabla_\beta (1/R)$

$T^{(3)}_{\alpha\beta\gamma}(R) = \nabla_\alpha \nabla_\beta \nabla_\gamma (1/R)$

Specializing to the dipole for two atoms at long range

$$\mu_z^{AB} = (9\hbar R^{-7}/\pi) \int_0^\infty [\, \alpha^A(i\omega)\, B^B(0,i\omega) - \alpha^B(i\omega)\, B^A(0,i\omega)\,]\, d\omega$$

$B^X(0,i\omega)$ denotes the dipole-dipole-quadrupole hyperpolarizability of atom X
$\alpha^X(i\omega)$ denotes the polarizability of atom X

If μ_z^{AB} is positive, the polarity of the dispersion dipole is A^+B^-

Each atom is hyperpolarized by the fluctuating charge distribution of the neighboring atom, and the applied field
The applied field alters spontaneous quantum fluctuations of the atomic charge densities

L. Galatry and T. Gharbi, *Chem. Phys. Lett*. **75**, 427 (1980).
K. L. C. Hunt and J. E. Bohr, *J. Chem. Phys*. **83**, 5198 (1985).

The Dispersion Dipole in *ab initio* Quantum Calculations for $H_2 \cdot \cdot \cdot H$

$$\mu^M(r, R, \theta) = 4\pi/3^{1/2} \sum_{\lambda, L, m} D_{\lambda L}(r, R) \langle \lambda\ L\ m\ M - m \mid 1\ M \rangle Y_\lambda^m(\theta, \phi)\, Y_L^{M-m}(0, 0)$$

D_{01} converges to the known long-range form!

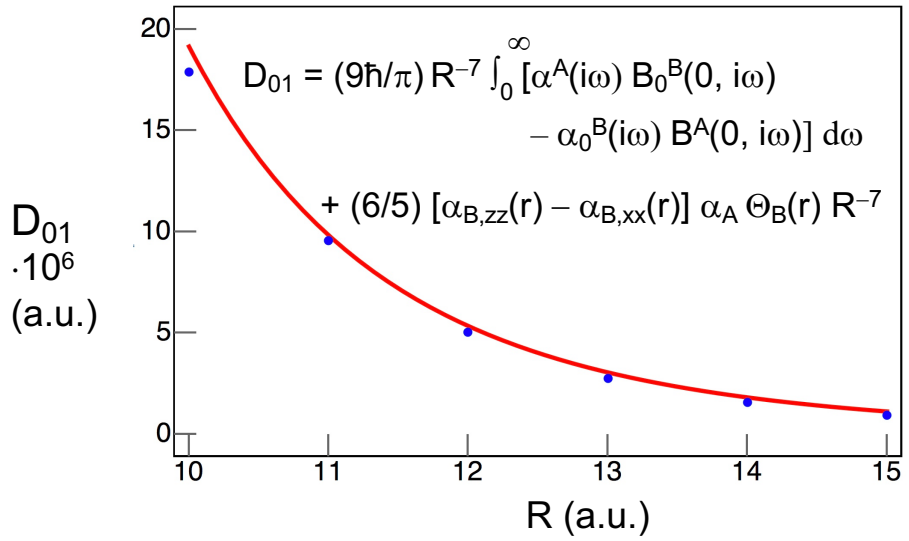

Dispersion plus back induction, aug-cc-pV5Z basis with correction for basis-set extension errors (BSSE)

Long-range analytical form: Bohr & Hunt (1987)
Values of the susceptibilities: Bishop & Pipin (1992)
Ab initio results: H.-K. Lee, X. Li, E. Miliordos, and K. L. C. Hunt, *J. Chem. Phys*. **150**, 204307 (2019).

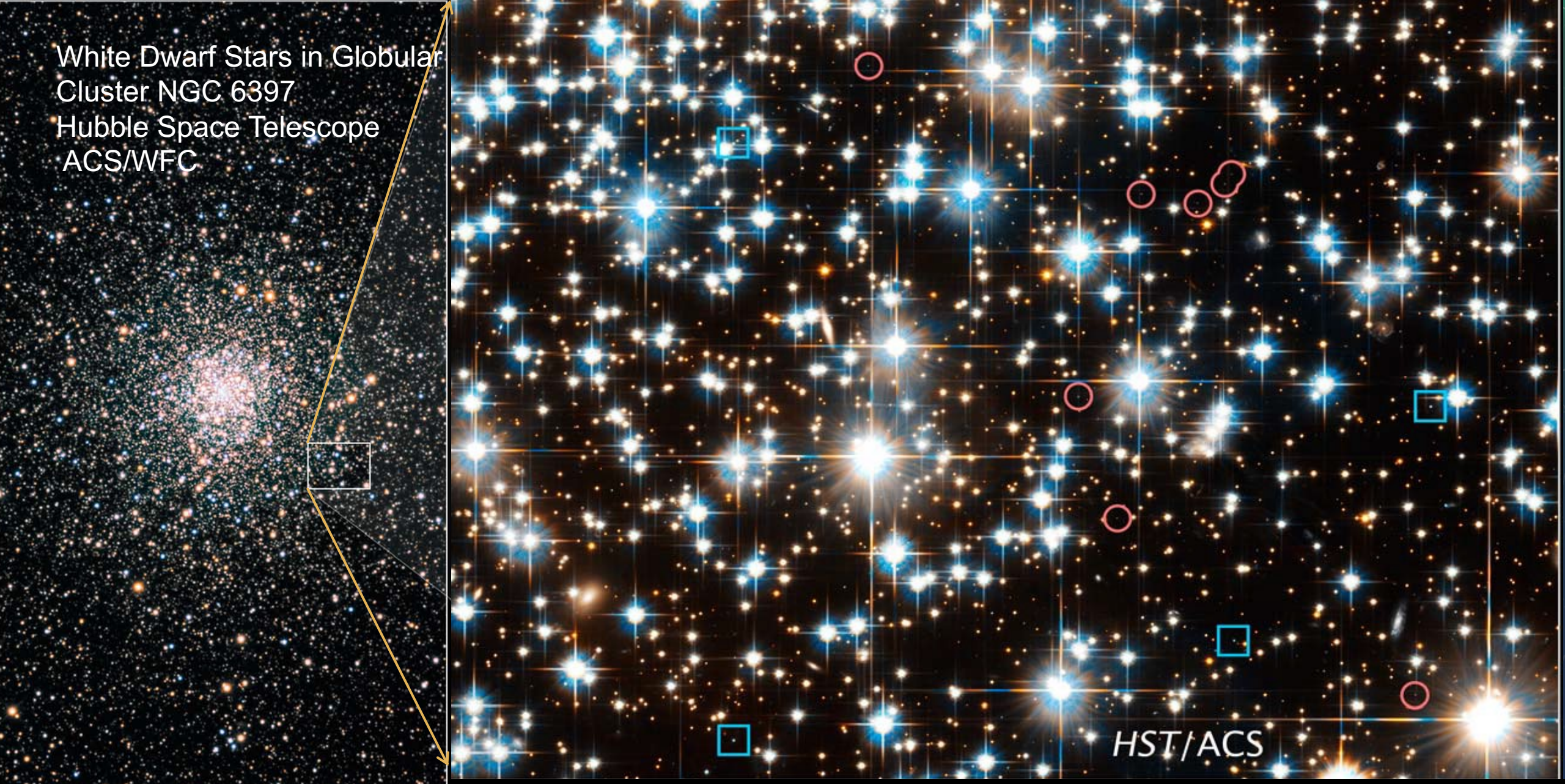

NASA, ESA, and H. Richter, University of British Columbia
STScI-PRC07-42

Astrophysical evidence for collision-induced absorption

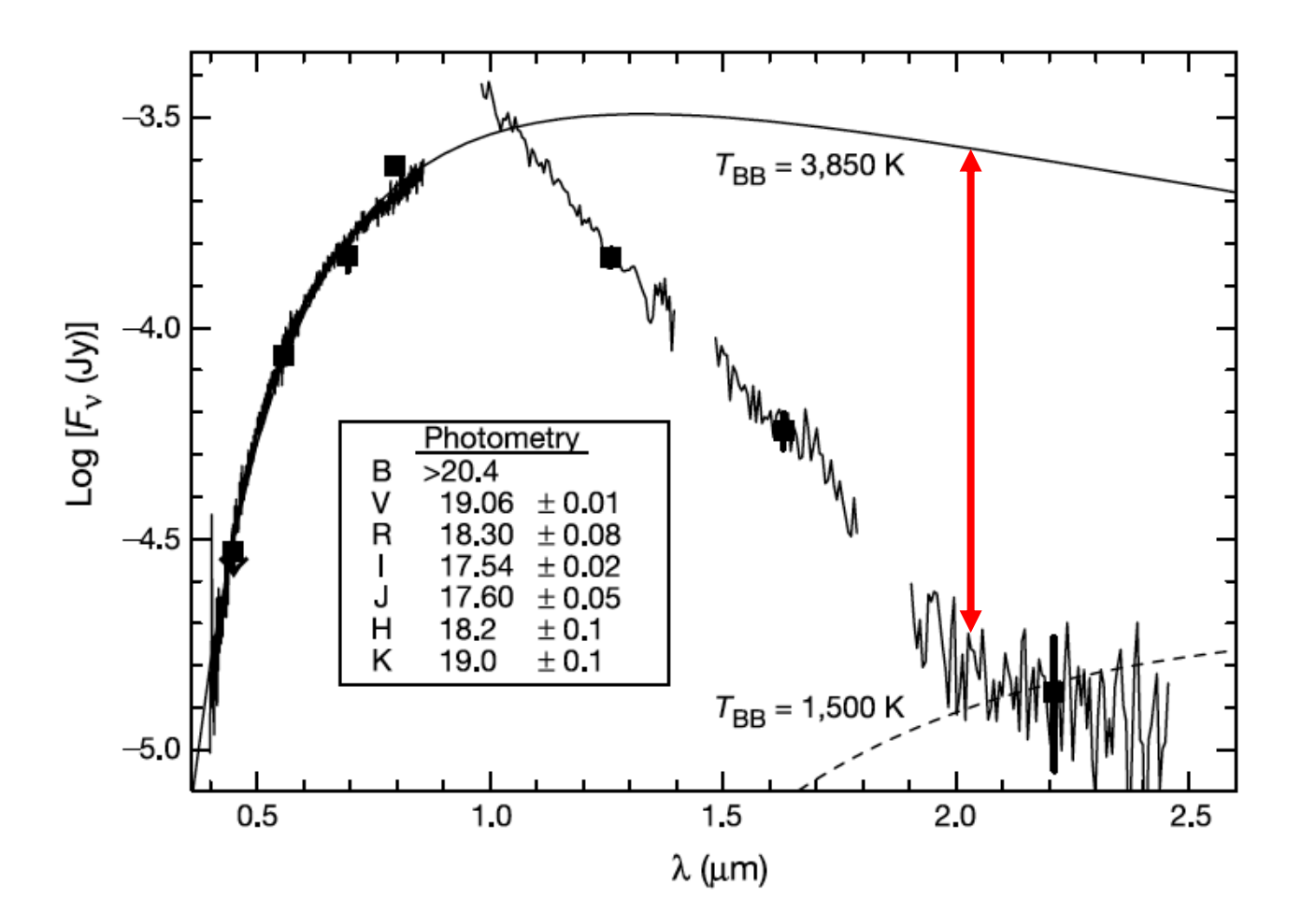

Observations of the cool white dwarf WD0346+246, with the Jacobus Kapteyn Optical Telescope, the UK Infrared Telescope, and the NIRC instrument (at the W. M. Keck I Observatory in Hawaii)

Estimated age: 12 billion years

Opacity due to collision induced absorption by H_2-H_2 and H_2-He increases by about 2 orders of magnitude in the range 1-2 μm.

Ratios of H_2 to He can be determined by detailed study of the IR spectrum.

S. T. Hodgkin, B. R. Oppenheimer, N. C. Hambly, R. F. Jameson, S. J. Smartt and I. A. Steele, *Nature* **403**, 57 (2000).

$H_2 \cdots H_2$: Comparison of our results with AUTOSURF results

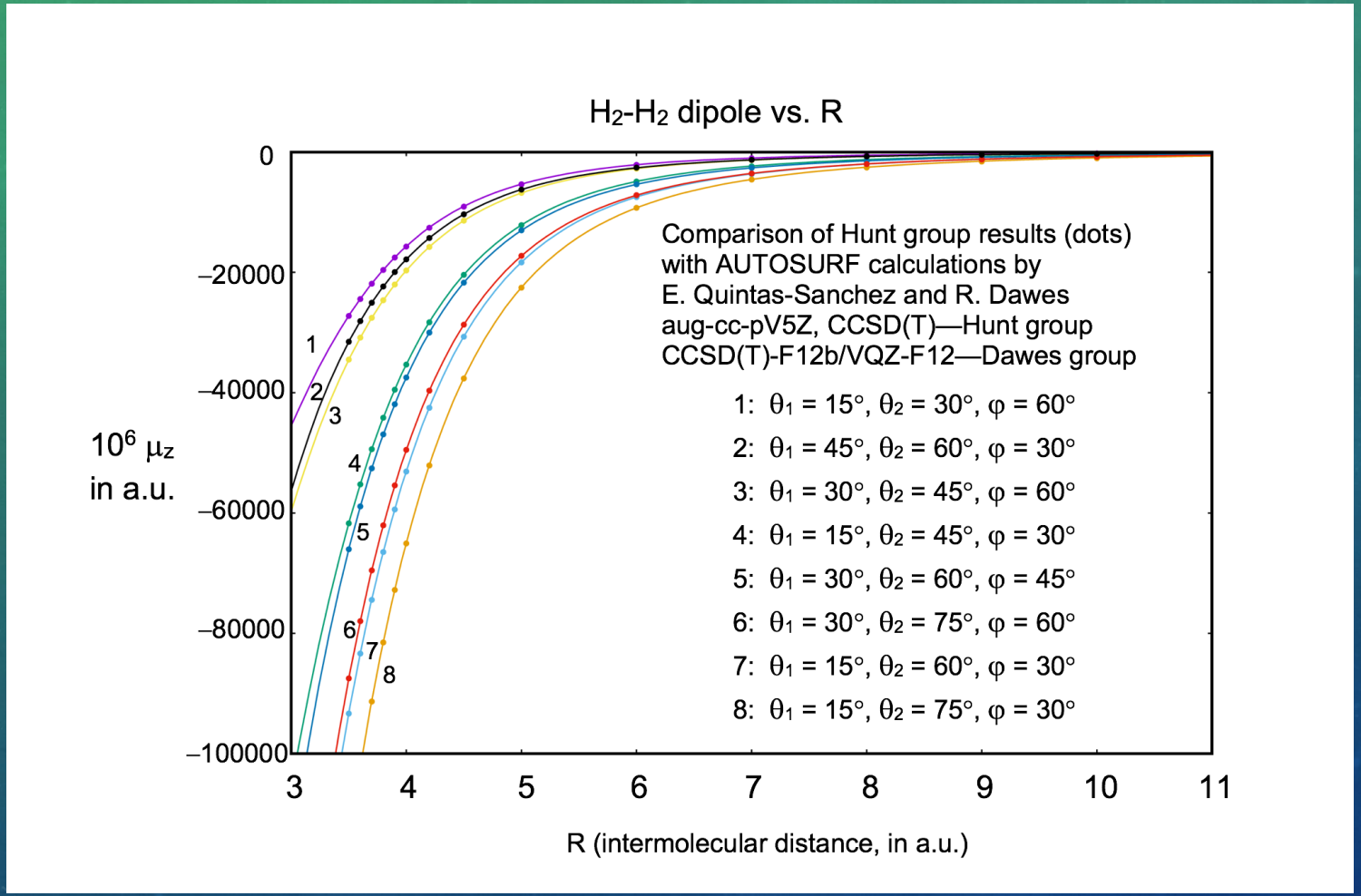

X. Li, A. Mandal, H.-K. Lee, E. Quintás-Sanchez, Evangelos Miliordos, R. Dawes, and K. L. C. Hunt, to be published.

Hunt Group, MSU

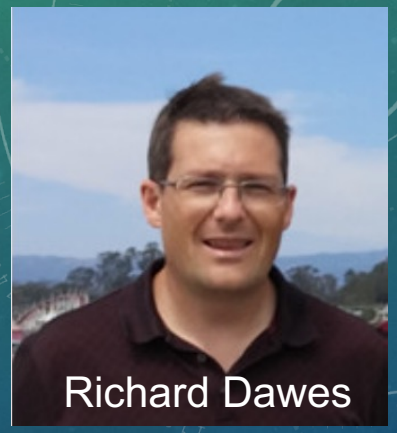

Dawes Group, Missouri University of Science and Technology

H_2-H_2: Comparison of our most recent work with previous calculations

New work: aug-cc-pV5Z basis, 320 (248) basis functions; spot-checked with aug-cc-PV6Z work
MFB/MBF/FZB: 62 basis functions

New work: Total of 27 (17) relative orientations, most with non-zero μ_X and μ_Z
MFB/MBF: 18 relative orientations, 9 non-redundant dipole components
FZB: 13 relative orientations

New and old work: Bond lengths r = 0.942, 1.111, 1.280, 1.449, 1.618, 1.787, 2.125, 2.463, 2.801 a.u., combined for 45 (36) pairs of bond lengths,
MFB/MBF: 4 pairs of bond lengths
FZB: 10 pairs of bond lengths

Nathan Jansen

New work: 24 (15) separations between the molecular centers of mass, from 3.4 a.u. to 10.0 a.u.
MBF: 9 separations

Method: Production runs with CCSD(T), but checked against CCSD(T)-F12 and full CI
This work: 6 field strengths to determine the collision-induced dipoles

MFB: W. Meyer, L. Frommhold, and G. Birnbaum, *Phys. Rev. A* **39**, 2434-2448 (1989).
MBF: W. Meyer, A. Borysow, and L. Frommhold, *Phys. Rev. A* **40**, 6931-6949 (1989).
FZB: Y. Fu, C. G. Zheng, and A. Borysow, *J. Quant. Spectrosc. Rad. Transfer*, **67**, 303-321 (2000).
This work: Nathan Jansen, Hua-Kuang Lee, X. Li, A. Mandal, E. Miliordos, and K. L. C. Hunt

Spherical Tensor Analysis for the $H_2 \cdots H_2$ dipole

Tensor components of the dipole are expressed in terms of the spherical harmonics of the orientation angles for the bond axes and the intermolecular vector

$$\Delta\mu^M(\mathbf{r}_A, \mathbf{r}_B, \mathbf{R}) = (4\pi)^{3/2}\, 3^{-1/2} \sum D_{\lambda_A\lambda_B\Lambda L}(r_A, r_B, R)$$
$$\times Y_{\lambda_A m_A}(\Omega^A)\, Y_{\lambda_B m_B}(\Omega^B)\, Y_{L\, M-m}(\Omega^R)$$
$$\times \langle\, \lambda_A\, \lambda_B\, m_A\, m_B \mid \Lambda\, m \,\rangle \langle\, \Lambda\, L\, m\, M-m \mid 1\, M \,\rangle$$

Summation runs over λ_A, λ_B, Λ, L, m_A and m_B

Spectroscopic implications

$$\Delta\mu^{M}(\mathbf{r}_A, \mathbf{r}_B, \mathbf{R}) = (4\pi)^{3/2}\, 3^{-1/2} \sum D_{\lambda_A \lambda_B \Lambda L}(r_A, r_B, R)\, Y_{\lambda_A m_A}(\Omega^A)\, Y_{\lambda_B m_B}(\Omega^B)\, Y_{L\, M-m}(\Omega^R)$$
$$\times \langle\, \lambda_A\, \lambda_B\, m_A\, m_B \mid \Lambda\, m \,\rangle \langle\, \Lambda\, L\, m\, M-m \mid 1\, M \,\rangle$$

If the potential is isotropic, then

- Coefficients $D_{\lambda_A 0 \Lambda L}$ produce transitions with $\Delta J^A = \pm \lambda_A$ and $\Delta J^B = 0$
- Coefficients $D_{0 \lambda_B \Lambda L}$ produce transitions with $\Delta J^A = 0$ and $\Delta J^B = \pm \lambda_B$
- Coefficients $D_{\lambda_A \lambda_B \Lambda L}$ with $\lambda_A \neq 0$ and $\lambda_B \neq 0$ produce *simultaneous* transitions with $\Delta J^A = \pm \lambda_A$ and $\Delta J^B = \pm \lambda_B$
- Higher ΔJ values produce absorption in the farther wings of the spectrum

Anisotropies of the potential combine with the angular momentum indices on the dipole coefficients to produce transitions with additional ΔJ values

Collision-induced absorption by $N_2 \cdots N_2$ at 78 K

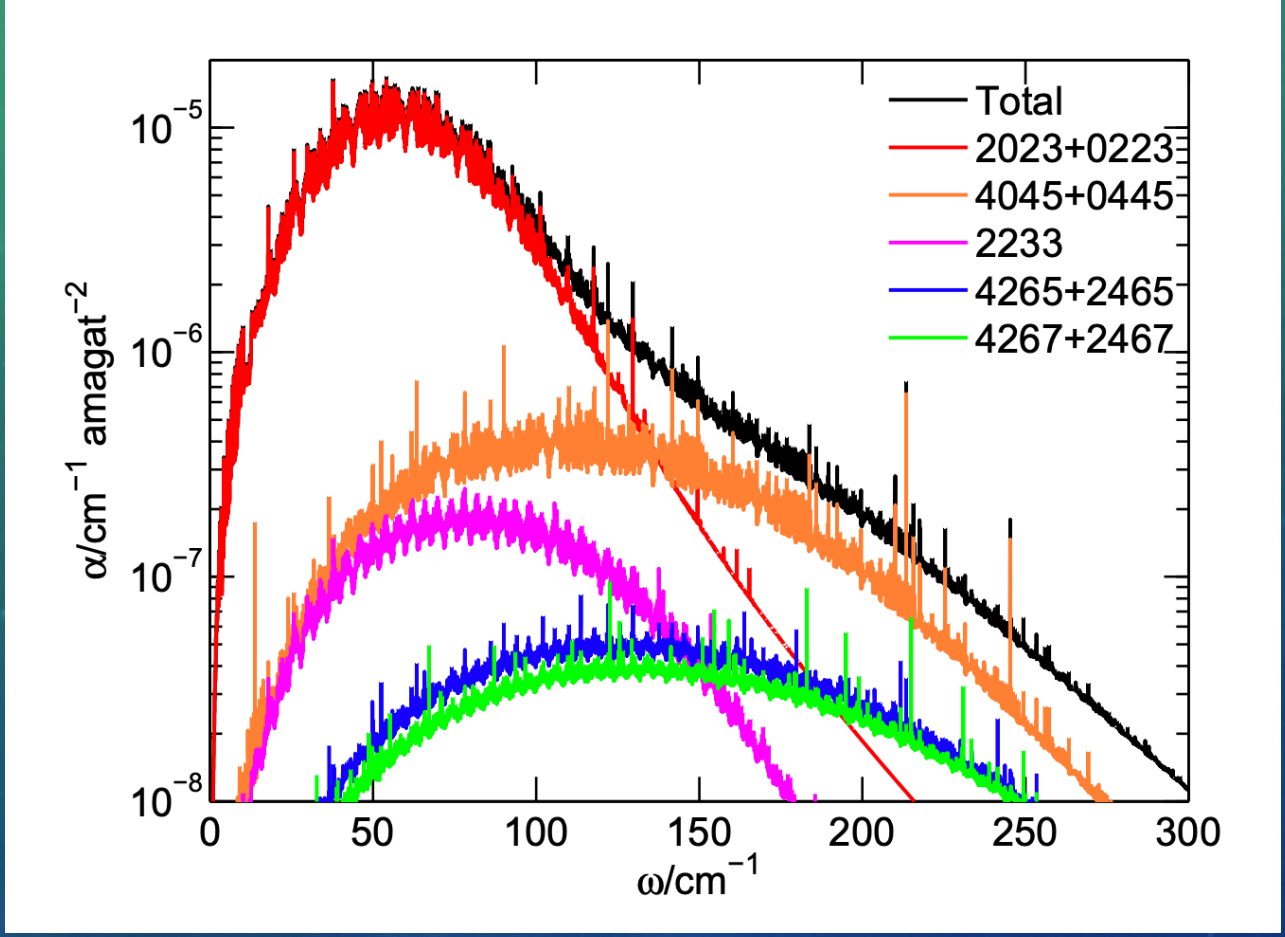

T. Karman, E. Miliordos, K. L. C. Hunt, G. Groenenboom, and A. van der Avoird, *J. Chem. Phys*. **142**, 084306 (2015).

Comparison of results for D_{2023} from various fits

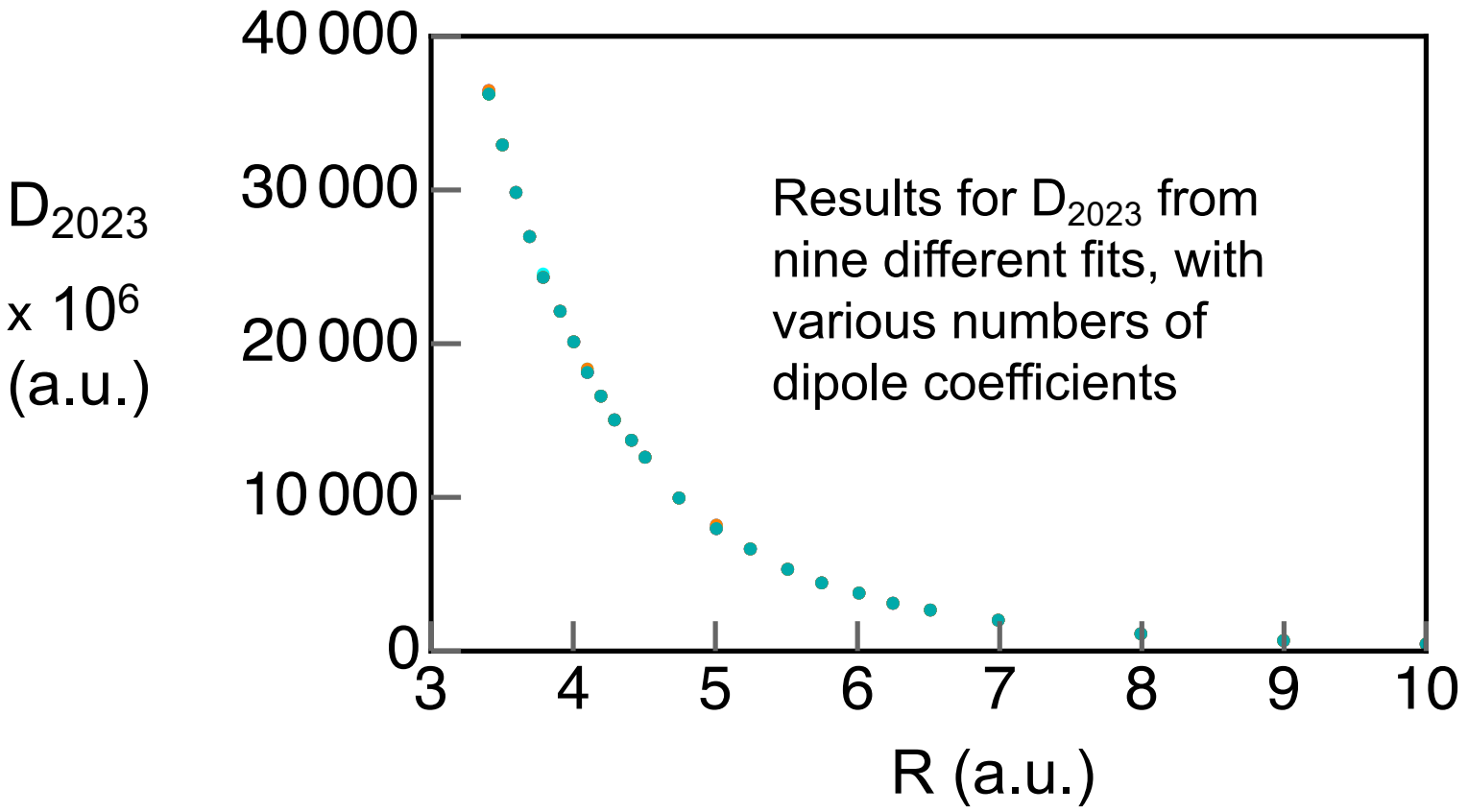

Comparison of results for D_{2023} with long-range forms

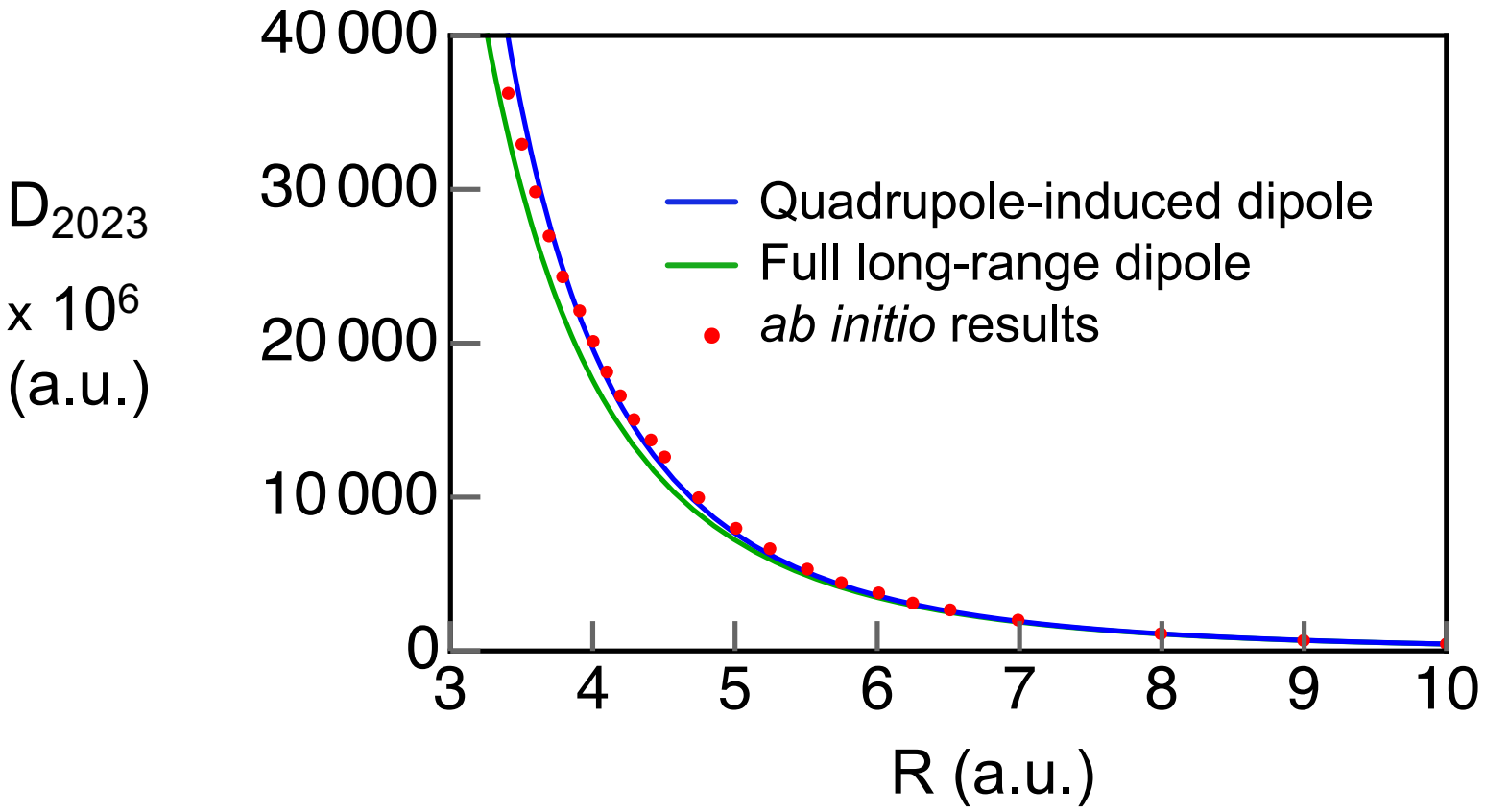

Comparison of results for D_{2233} from various fits

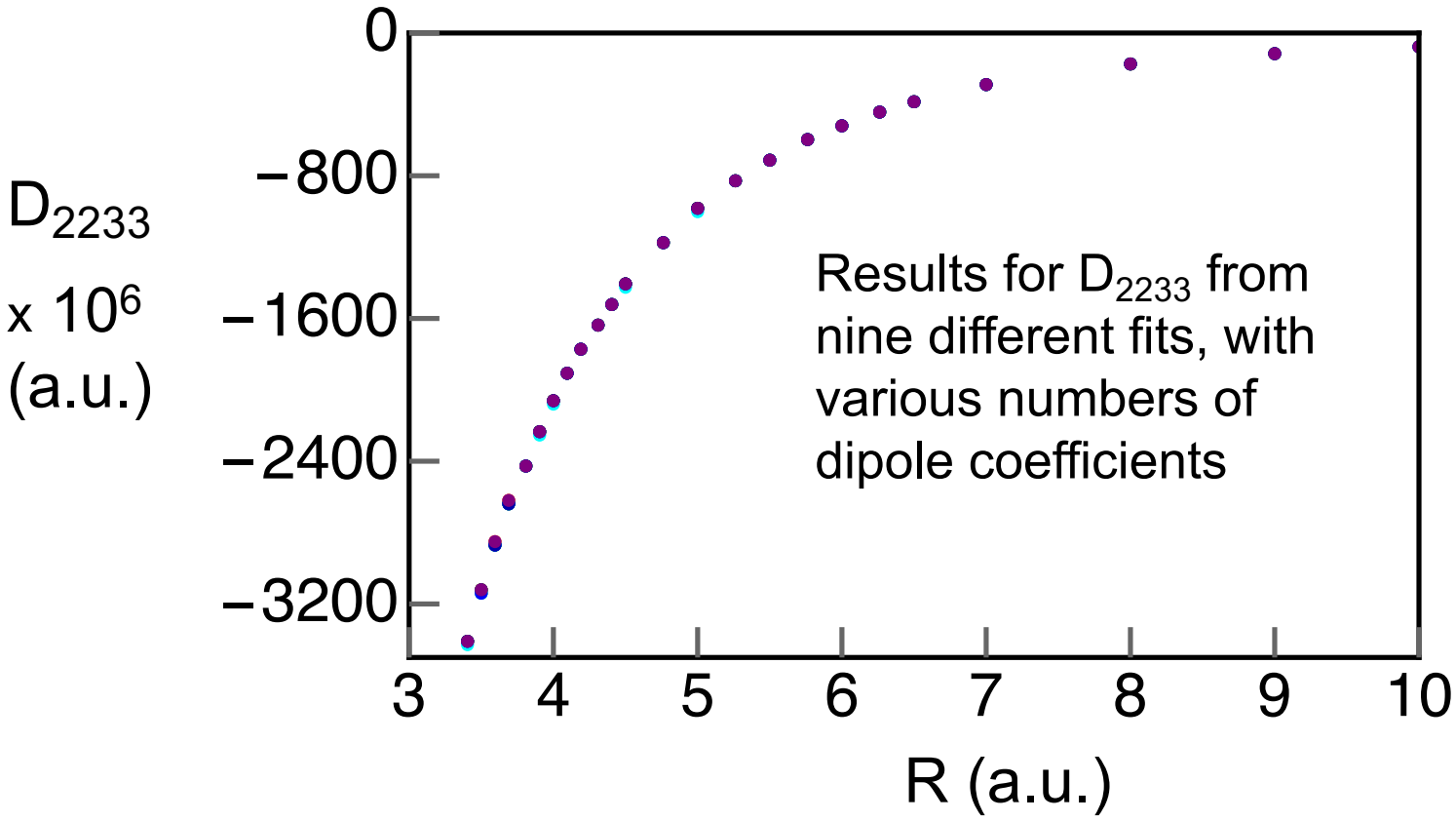

Comparison of results for D_{2223} with long-range forms

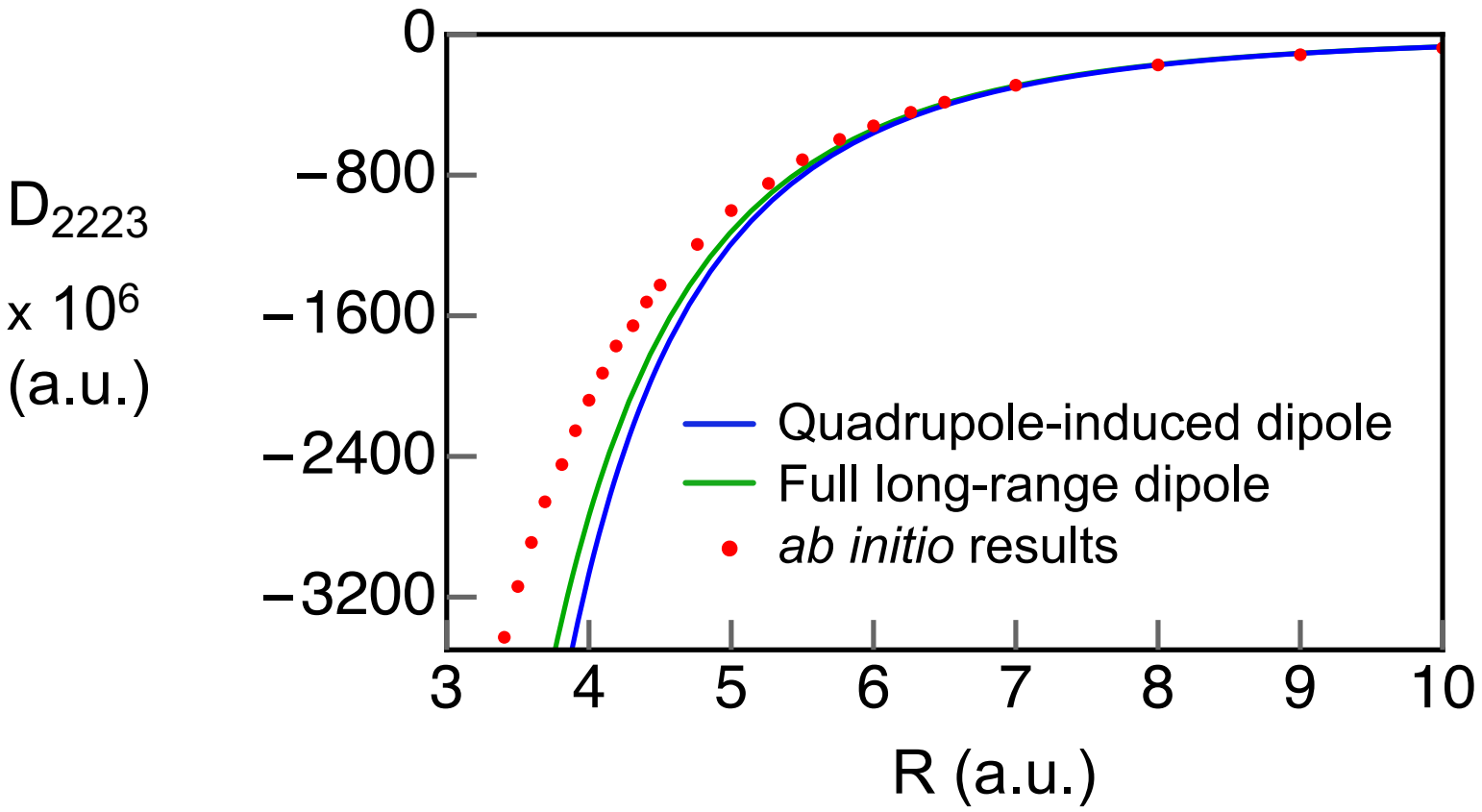

Comparison of results for D_{4045} from various fits

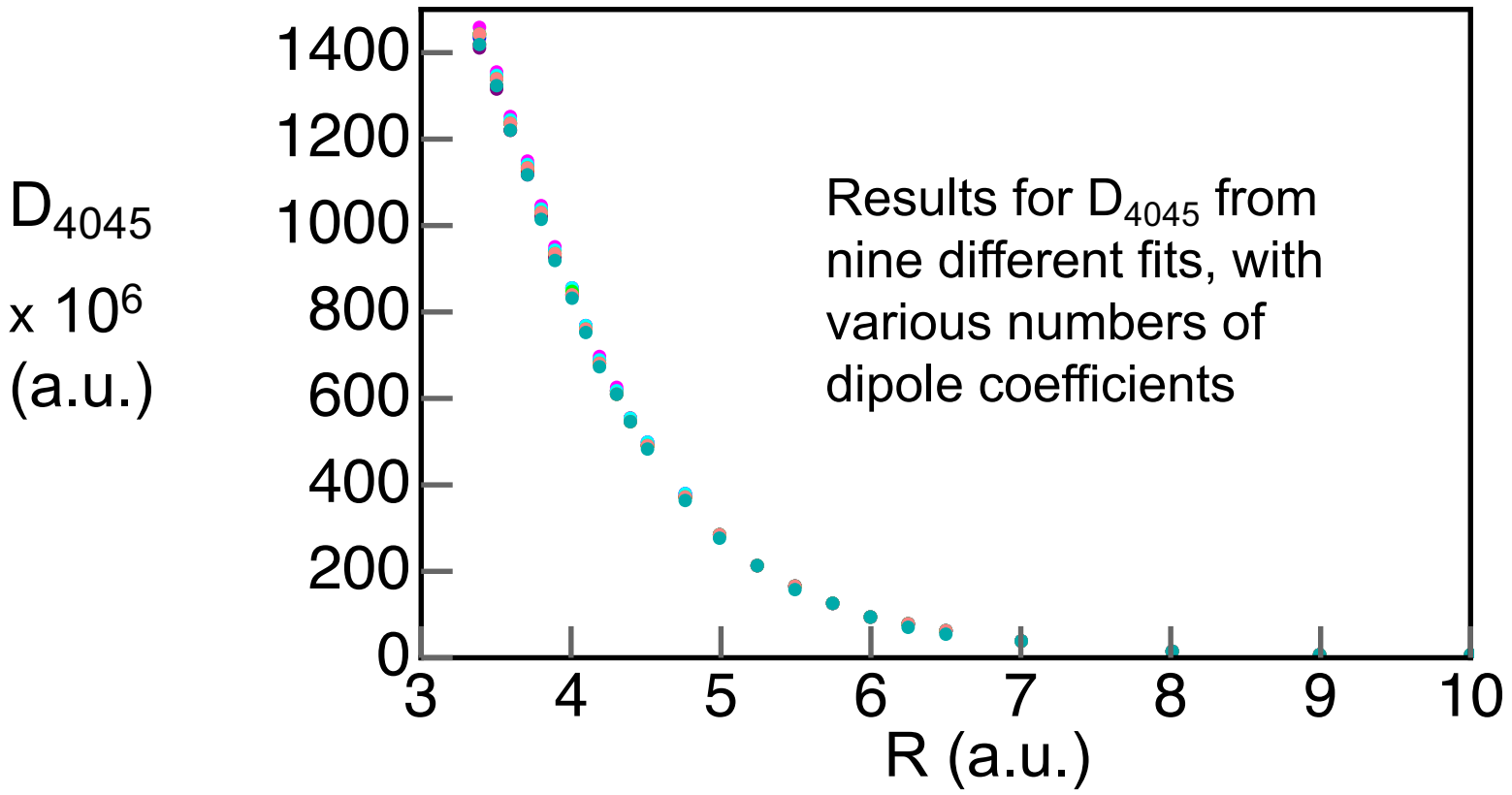

Comparison of results for D_{4045} with long-range form

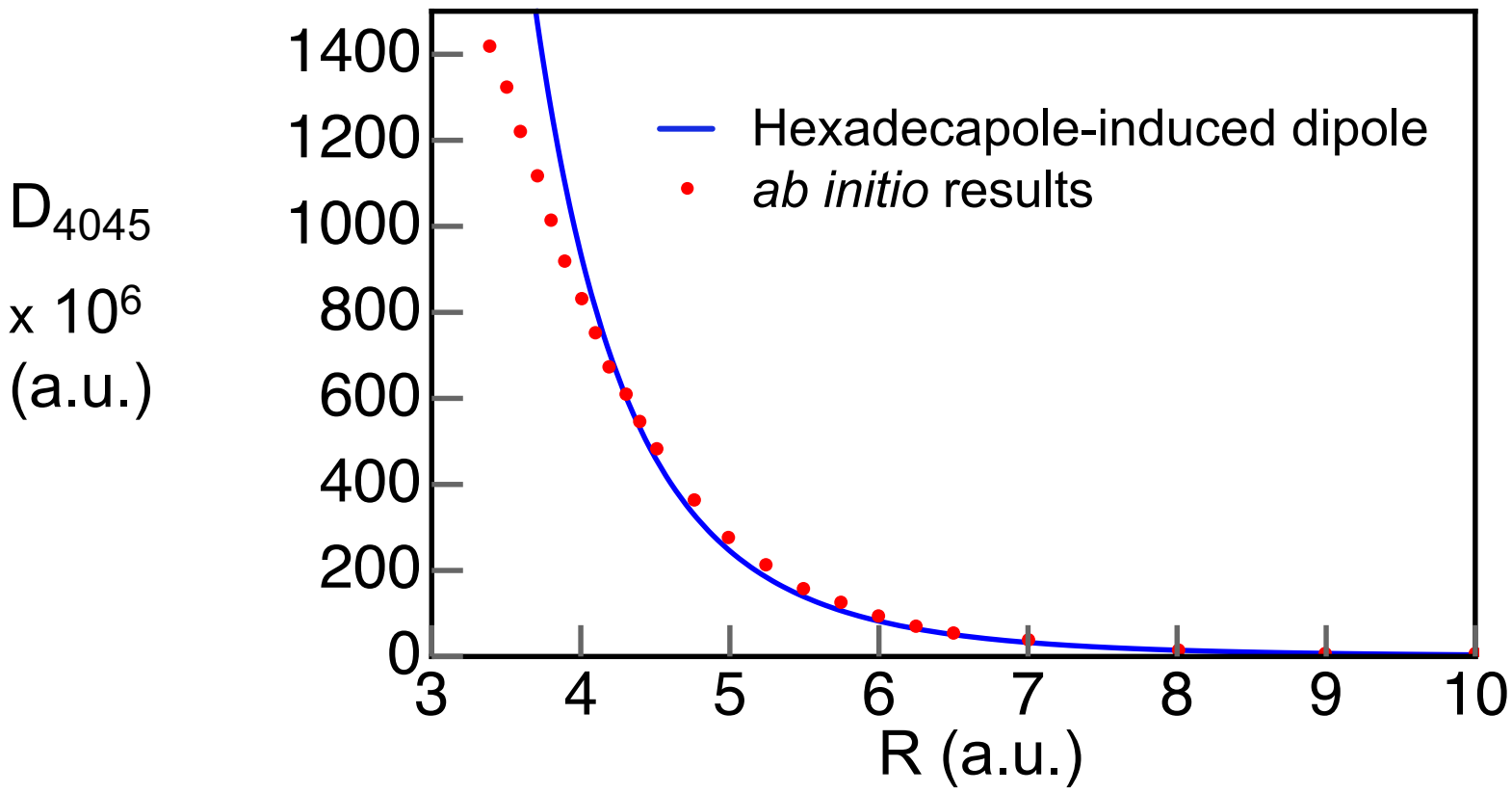

Comparison of results for D_{4245} from various fits

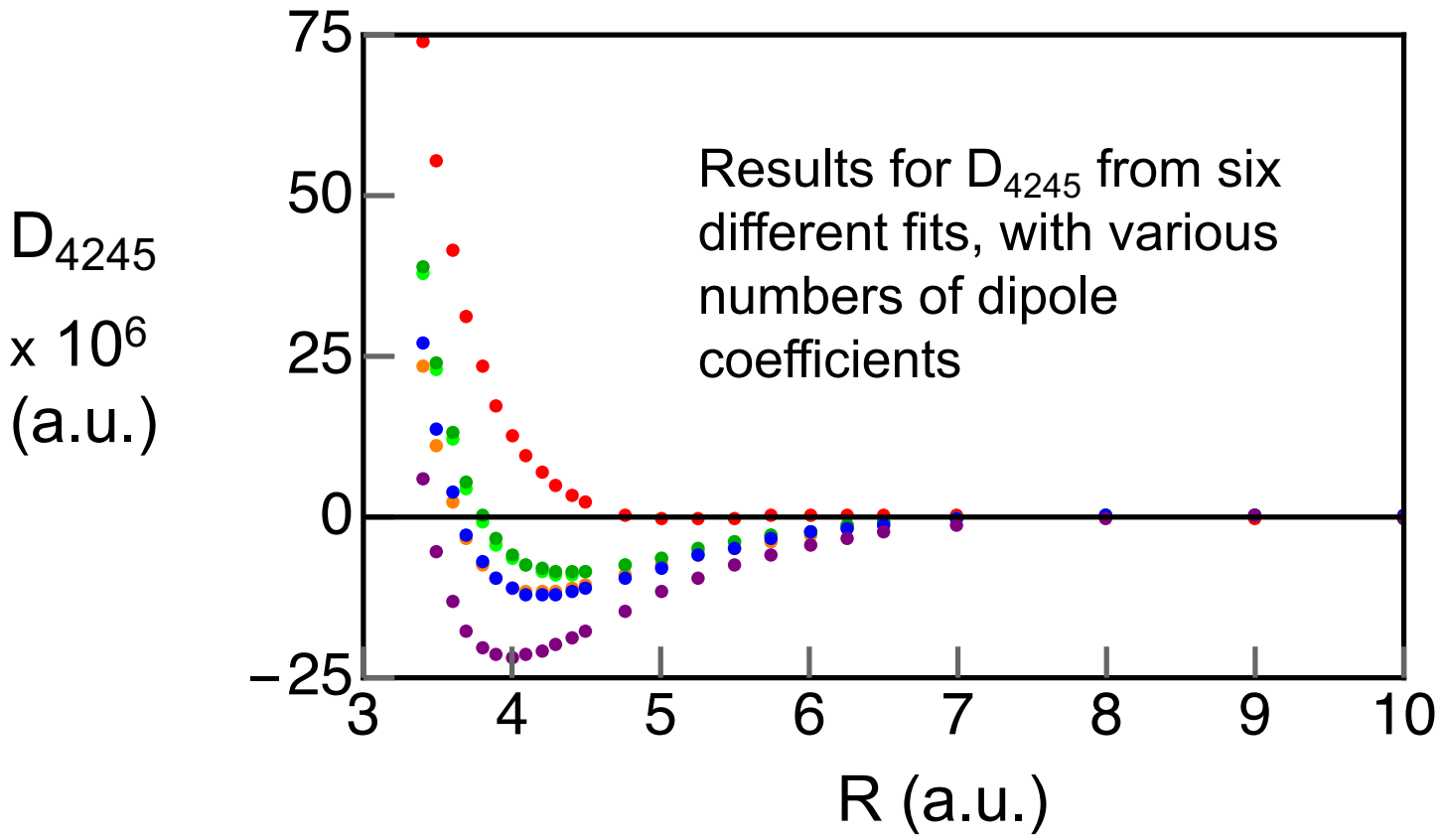

Comparison of results for D_{4245} with long-range form

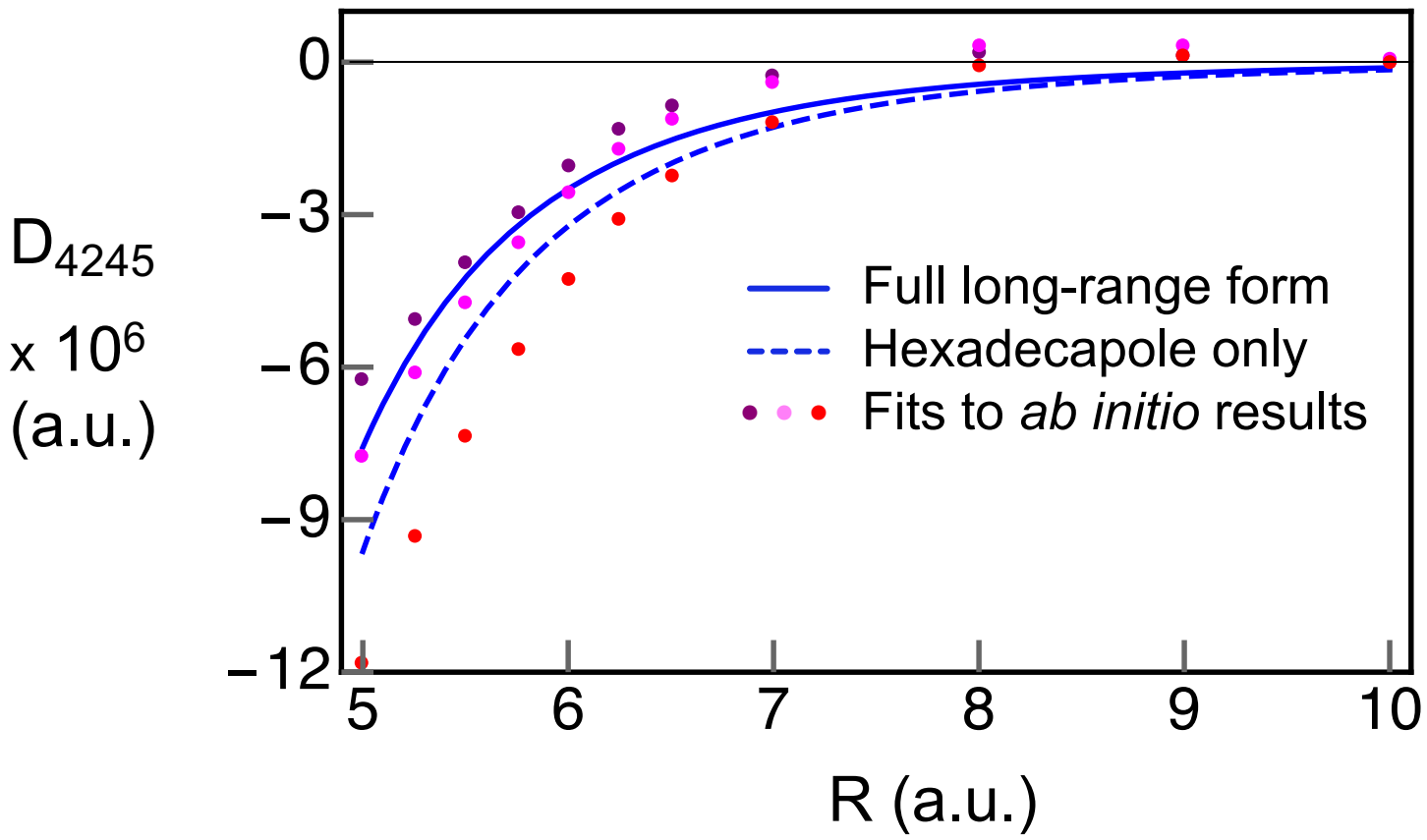

Hydrogen molecule potential and vibrational energy levels

Vibrational levels from J. D. Poll and G. Karl, *Can. J. Phys*. **44**, 1467 (1966).

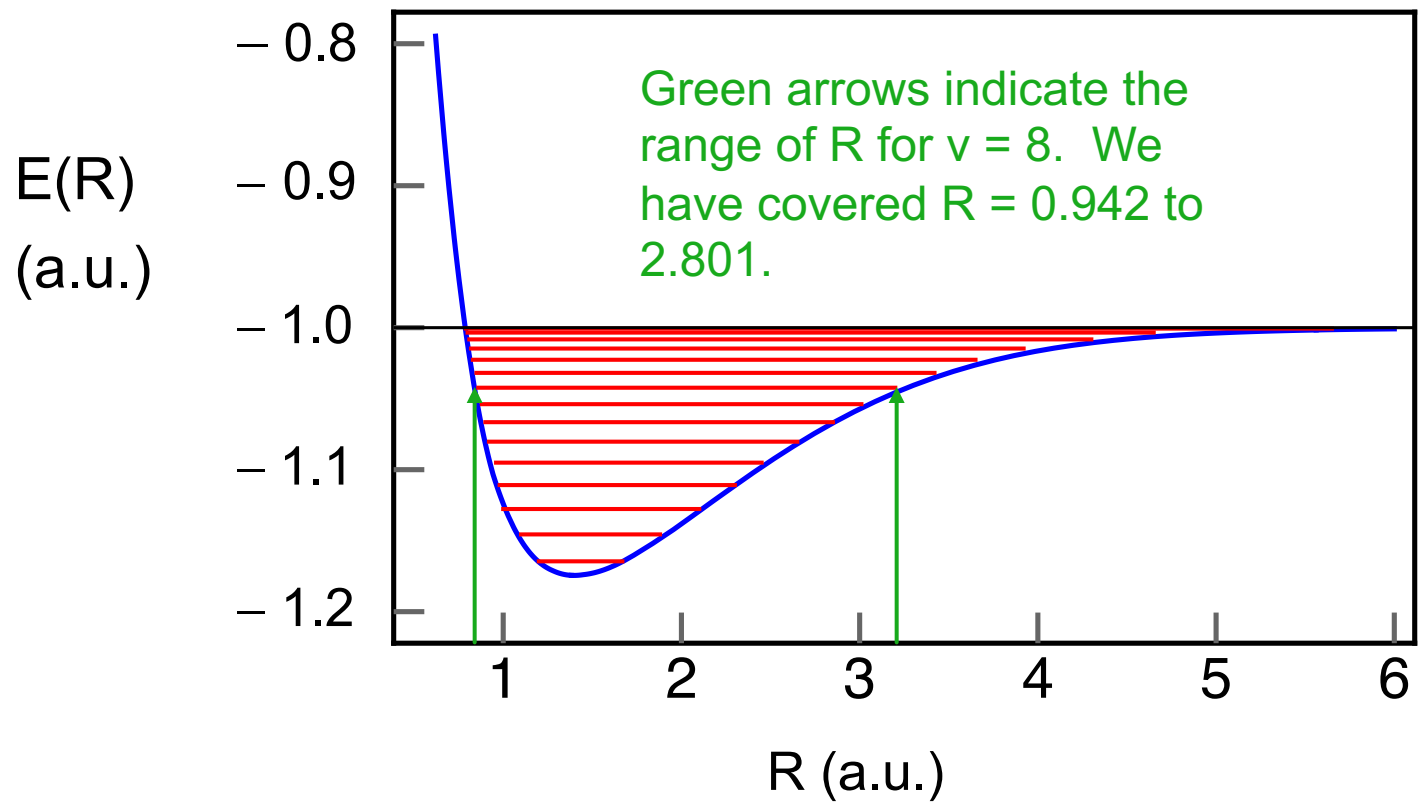

Exploration of contributions to the force from all orbitals and analysis of exchange effects: In progress

Desirability of adopting a Slater basis?

Difference between the charge density in the 1s state of the H atom and the representation with [9/6] Gaussian s functions

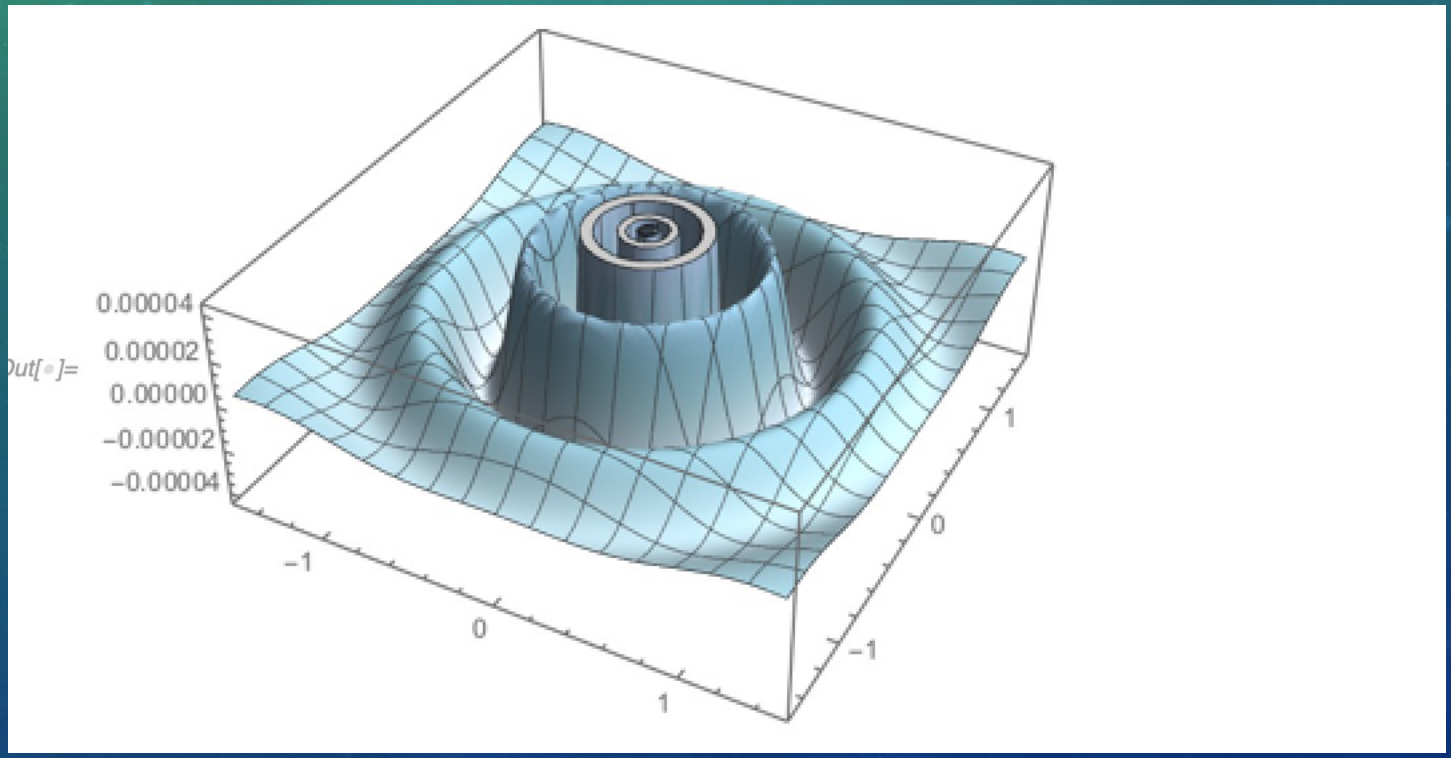

Collision-induced three-body polarizability of helium

Jakub Lang, Michał Przybytek, Michał Lesiuk, and Bogumił Jeziorski

https://doi.org/10.1063/5.0137879

- Coupled-cluster and full CI calculations of the three-body polarizability of helium, used to determine the third dielectric virial coefficient
- Comparison with experimental data and with Path Integral Monte Carlo calculations by Giovanni Garberoglio, Allan H. Harvey, and Bogumił Jeziorski
- Important result for quantum metrology, eliminates the main accuracy limitation in the optical pressure standard

“tanquam ex ungue lionem,” Johann Bernoulli about Isaac Newton

Dr. Anirban Mandal

Prof. Evangelos Miliordos (Auburn)

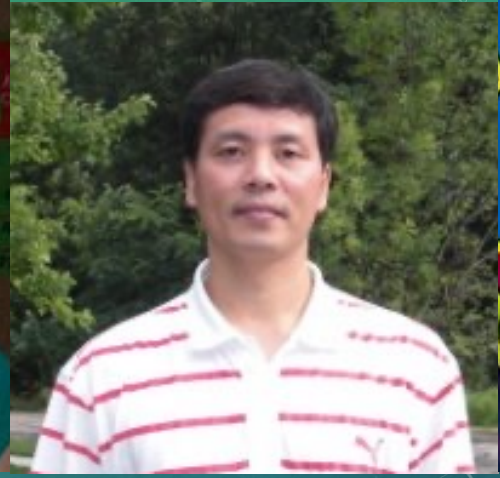

Dr. Janelle Bradley | Dr. Xiaoping Li | Dr. Sasha North

Nathan Jansen | John Buhl | Sara Jovanovski

Dr. Hua-Kuang Lee

Garrett Mai, Ashley Siegmund, Scott Gilbert, Corbin Fleming-Dittenber, Zyk Hlavacek, Drew Scheffer, Jessica Messing, Aidan Gauthier, Matt Loucks, [David Wang, and Julia Egbert]

Nathan Jansen will present a poster on the entropies of Schrödinger's cat states on quantum computers.

Acknowledgments:
National Science Foundation Grant CHE-1900399
National Science Foundation Grant CHE-2154028

Thanks for the invitation to give this seminar!

Thanks for Letters of Collaboration from:

Prof. Ben Levine
Stony Brook

Prof. Richard Zare
Stanford

Prof. Elad Harel
MSU

Prof. Warren Beck
MSU

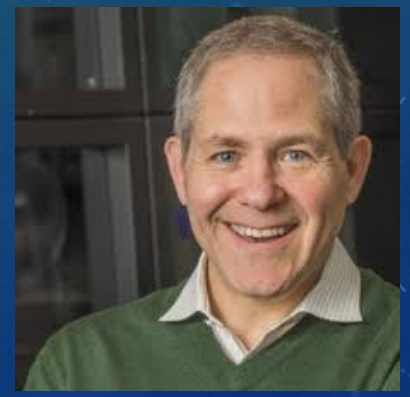

Prof. Marcos Dantus
MSU

I am very grateful to the Institute for Advanced Studies of the University of Luxembourg for a DISTINGUISHED grant, which has made my visit possible, and to Professor Jens Kreisel, Rector of the University of Luxembourg, Professor Catherine Léglu, Vice-Rector for Academic Affairs, Professor Claus Vögele, Dr. Sylvie Fromentin, Paula Souza, and Manuel Quaino, F. M. and Logistics Officer.

Very special thanks are due to Professor Alexandre Tkatchenko, Head of the Department of Physics and Materials Science, Professor Aurélia Chenu, Professor Susanne Siebentritt, Dr. Dmitry Fedorov, Dr. Ashmita Bose, Dr. Ariadni Boziki, Dr. Dahvyd Wing, Dr. Matteo Gori, Dr. Dhruv Sharma, Dr. Jorge Alfonso Charry Martinez, Dr. Gregory Cordeiro Fonseca, Dr. Szabolcs Góger, Dr. Igor Poltavskyi, Dr. Josh Berryman, Kyunghoon Han, Matyas Nachtigall, Mirela Puleva, and all additional graduate students and postdoctoral researchers in the Tkatchenko research group. I am also very grateful to Dr. Elodie Duriez and Yolande Edjogo!